The Synthesis of Novel Conducting Polymers and Oligomers for Use in Electrical Devices, Drug Delivery Systems, and Energy Dynamics Studies

The Thesis Committee for Monica Irais Villa
Certifies that this is the approved version of the following thesis:

The Synthesis of Novel Conducting Polymers and Oligomers for Use in Electrical Devices, Drug Delivery Systems, and Energy Dynamics Studies

APPROVED BY
SUPERVISING COMMITTEE:

Supervisor:

Bradley J. Holliday

Richard A. Jones

The Synthesis of Novel Conducting Polymers and Oligomers for Use in Electrical Devices, Drug Delivery Systems, and Energy Dynamics Studies

by

Monica Irais Villa, BA, BA

Thesis

Presented to the Faculty of the Graduate School of

The University of Texas at Austin

in Partial Fulfillment

of the Requirements

for the Degree of

Master of Arts

The University of Texas at Austin

May 2010

Dedication

First and foremost, I dedicate this to my mom Mayela Rutiaga, without whom I would be nothing. I am eternally grateful to my sister Roxanna Villa for the endless laughs and shopping trips, to Travis Hesterberg for making every workday memorable and of course to my fiancé Eric Gardner for making me whole. I could not have remained (almost) sane in grad school without the unfaltering aid of my closest friends and family, all of whom made chemistry possible even during the toughest times.

Acknowledgements

The research described herein was funded in part by a grant from the American Heart Association and funding through the Department of Energy sponsored Energy Frontier Research Center (EFRC). It was performed under the invaluable direction of an incredible advisor, Bradley Holliday.

April 29, 2010

Abstract

The Synthesis of Novel Conducting Polymers and Oligomers for Use in Electrical Devices, Drug Delivery Systems, and Energy Dynamics Studies

Monica Irais Villa, M.A.

The University of Texas at Austin, 2010

Supervisor: Bradley J. Holliday

Described herein are three projects centered on the synthesis of conducting polymer derivatives for various applications. The first is the novel synthesis of 9,9-dioctylfluorene-*co*-benzothiadiazole [F8BT] oligomers through solid phase synthesis for the study of the thermodynamics and kinetics of electron transfer in the polymer. The second endeavor involves the synthesis of a series of 4”,3’’’-dialkyl-2,2’:5’,2”:5”,2’’’:5’’’,2’’’’:5’’’’,2’’’’’-sexithiophenes for the studies on crystal packing and surface deposition of organic p-type semiconducting materials. Lastly is described the development of a conducting metallopolymer based on the ligand 2,6-Bis(4-(2,2’-bithiophen-5-yl)-1*H*-pyrazol-1-yl)pyridine for use in a drug delivery system.

Table of Contents

List of Tables

List of Figures

List of Schemes

Introduction

ORGANIC SEMICONDUCTING MATERIALS

Theory and Structure

Organic semiconductors have gained wide popularity in research and development of new technology due to their promising electric and optical properties. These materials form a bridge in conductivity between metals and insulators, and thus became target compounds for the replacement of metals in various electronic devices. The crystal lattice structure of a metal allows for an overlap of orbitals, which in turn spreads the discrete energy levels into conductive energy bands. The width of the bands is determined by the size of this overlap. In a similar fashion, delocalization of electron density in organic semiconducting materials, possible through extended bonding, creates a band system through which conduction can occur. Within these bands, electrons can move within a wave function close to that of free electrons.[1]

While the energy bands of metals do not have a discrete band separating conduction, insulating compounds have large gaps that make conduction energetically unfavorable and unlikely. Organic semiconductors lie in between the two extremes, so excited electrons must jump a certain energy gap in order to be conducted throughout the compound (Figure 1). The conduction band energy is based on the electron affinity of the material and is tied to the lowest unoccupied molecular orbital (LUMO).[2] Conversely, the ionization potential corresponds to the valence band and highest occupied molecular orbital (HOMO). On average, semiconductors have bandgaps of 1-3 eV. The band gap and width (or energy) are in turn directly determined by the degree of π orbital overlap along the chain.[3]

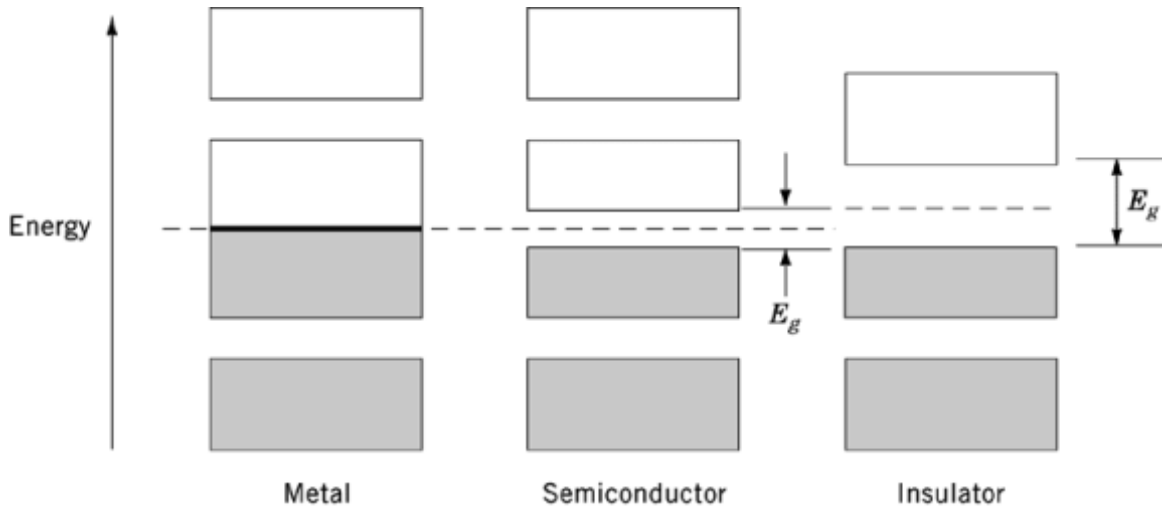

Figure 1. General energy diagrams for metals, semiconductors, and insulators.[4]

Conductive polymers (CPs) have become the standard in current conducting materials. After the finding of high conductivity in polyacetylene when doped with iodine,[5] this CP became the most widely studied in the field of semiconducting applications, despite its insoluble, highly crystalline, and unstable nature.[6] Other prevalent polymers include polyacetylene, polyaniline, polypyrrole, and paraphenylene.[7] The electronic activity of these and other CPs have made them viable materials in a multitude of electronic applications such as thin-film transistors for flat panel displays and radio frequency identification tags.[8] Conductive polymers hold many advantages over inorganic materials, such as ease of processability, low cost of manufacturing, and an increase in conductivity with increasing temperature.[9] Their application is prevalent in light-emitting diodes and photovoltaic devices, such as in emissive displays, plastic electronics, and photocells for imaging and solar energy conversion.[10]

For the progress of organic electronics, semiconducting materials must have high charge-carrier mobility which can be optimized through understanding and control of their microstructure and nanostructure.[11] The mobility of charges in small organic

molecules is based on a hopping mechanism due to their small π overlap, whereas the extended conjugation and degree of order in CPs allows for high mobility through and between polymeric chains.[12] Thus, CPs are effectively wide gap semiconductors, displaying the same allowed absorption or emission at the band edge as semiconducting small molecules, but with higher charge mobility.

The semiconducting or conducting properties of CPs are induced by doping, whereas most are generally insulating in the undoped form. In doping, an electron is removed from the valence band or an electron is added to the conduction band; either path results in a large increase in conductivity. This can be done chemically or electrochemically, and it produces local carriers that can exist in many forms: cations, cation radicals, anions, anion radicals, dications, or dianions. At increasing doping levels, absorption in CPs at lower energy increases, and the edge of the band gap becomes obscured.[6]

When electrons have been excited from the valence band into the conduction band, the material is left with partially unfilled orbitals. The positively charged vacancy left behind is the carrier termed a "hole." The recombination of holes and electrons forms excitons. If the excitons are formed in the singlet state, they will radiatively decay through fluorescence; from the triplet state (formally forbidden by the requirement of spin conservation) they may radiatively decay to the ground state through phosphorescence.[13,14] If there should be an extra electron in the conduction band, the resulting geometry change will force an area of localization through significant lattice reorganization,[15] and this is termed a "polaron." A polaron can also translate into conduction by its movement through the polymer chain. The energy difference between the excited state and the ground state will determine the color of light emitted from a CP.[2]

Studies have revealed differences in the functionality of various conducting polymers. In order to maximize the utility of each CP, devices are often built with a blend of polymers, or complementary monomers are copolymerized to create a specialized material. Either avenue results in a material customized for a specific purpose. Blends and copolymers of this nature have been synthesized for better charge mobility, color tuning, and other desirable characteristics. Polymer blends in semiconducting devices are often made to have one component effective in charge transport, and one in luminescence.

Synthesis

CP research is often focused on the understanding of structure/property relationships,[16] resulting in the undertaking of a multitude of synthetic pathways of these compounds. Preparations vary from polymer to polymer and depend on the ultimate goal of the researcher, but given their basic need for a backbone of aromatic rings, routes for ring coupling and aryl-aryl bond formation such as Suzuki-Miyaura, Stille, Ullman, and Heck preparations are common. Rigid and planar structures are often sought due to their involvement in increasing the mobility of excited electrons. Coplanarity thus leads to better electrical properties and nonlinear optical properties.[3]

Researchers also attach to CPs various forms of alkyl chains for the sake of increasing solubility of high molecular weight polymers in common organic solvents. Variation in substitution can lead to changes in solvatochromism, thermochromism, and band gap size of the polymer.[17] The former two properties are due to rotation of neighboring aromatic rings, which leads to a decrease of π conjugation, changing the electronic structure responsible for the color changes.[18] Experimentation of morphology has thus resulted in employing substituents such as bulky alkyl and phenyl groups, and an assortment of electronegative groups. Studies have also shown a direct correlation

between morphology of semiconducting films and charge carrier mobility.[8] The synthesis of oligomers often takes place as an iterative coupling of monomers, and is undertaken for the purpose of bypassing high polydispersity and insolubility of many polymers. It is also used for the purpose of performing various conductive and morphology studies that can provide valuable information about the corresponding CP.

Polymerization can be performed chemically or by electrochemical means. An electrochemical cell, often under inert atmosphere due to the high oxygen and water sensitivity of many polymers, directly creates thin films. The cell contains a cathode, anode, substrate, and electrolyte solution. Often, the transparent conducting material indium-tin-oxide (ITO) is used as the substrate because its excellent injection of holes also makes it an optimum anode. The cathode, in turn, should be an electronegative metal in order to inject electrons effectively.[13] Polymer thin films can also be spin-coated onto the substrate, an approach that is advantageous in the deposition of homogenous films with controlled thickness.

Conducting polymers are processed into thin films for the purpose of characterization studies and implementation in various devices. One advantage of organic semiconductors is the amorphous nature of their films, which allows for deposition onto rigid or flexible substrates. However, thin films can still reflect the crystalline to amorphous nature of the fabricated polymer. For the purpose of device fabrication, CPs are often spin-coated onto the electrodes. Methods of fabrication, nature of substrates, structure of individual units, and choice of solvent all play a role in the solubility, molecular packing and morphology of thin films. Any surface treatment of the substrate and/or post deposition treatment with solvent vapors or heat can directly affect the molecular order of polymer thin films.[10] Even the varying conductivity of the ITO can affect device performance, since its non-stoichiometric nature forces its electronic

properties depend on preparation and cleaning methods.[2] In electrochemically deposited thin films, morphology of the polymer has been shown to reflect the type of substrate onto which it is deposited. Care must be taken, therefore, when choosing substrates for electrodepositing CPs bound for device use. For the purpose of morphological studies, different substrates have been used to study the effect of substrate composition on CP morphology and conductivity.[8] For example, treating silicon oxide, the most commonly used dielectric in thin-film transistors, with hydrophobic agents has been shown to triple charge carrier mobility.

Analysis

The techniques used to characterize conducting polymers are aimed at revealing details of identity, monodispersity, thermo- and photo-stability, electrochemistry, and fluorescence. The common techniques of ^{1}H and ^{13}C NMR, UV-Vis, Raman FT-IR, mass spectrometry, and infrared spectroscopy can be used to confirm the identity of CPs. Studies such as photoelectron spectroscopy, scanning probe microscopy, electrochemical techniques such as cyclic voltammetry and hybrid techniques such as spectroelectrochemistry, electrochemical quartz crystal microbalance studies, and photocurrent spectroscopy are used to procure information about conductance and optical characteristics. Photoelectron spectroscopy (X-ray or ultraviolet) is especially beneficial in studying the surface of bulk materials in a nondestructive approach.[17] Electrical impedance spectroscopy can be used to measure charge transport. Molecular modeling is also crucial in predicting conductive properties of CPs. In particular, *ab initio* calculations, which are based on first principles prior to empirical data, have become crucial to computing models for systems of small to medium size (<200 atoms).[19] Numerous methods are employed, and what distinguishes them is which electrons and orbitals are included in the calculations. Essentially, they quantify of the presence and

magnitude of neighboring electron influence. This property is one that can distinguish substances from each other. Likewise, ubiquitous density functional theory (DFT) can shed light on electronic structure, and particularly that of the CP ground state.

Electrochemistry is a particularly powerful instrument of characterization. The efficiency of charge injection and the degree of charge transfer will have an effect on the energies of the HOMO and LUMO levels of the CP. The potentials required for oxidation and reduction of the material can help characterize the HOMO and LUMO, respectively. Thus, the redox potentials found through electrochemistry are a direct measure of the energy of a CP's band gap.

LIGHT-EMITTING DIODES

Theory and Design

Emission of light caused by an applied electric field was first reported by C. Pope *et al*., in 1963, who saw electroluminescence from anthracene crystals placed between Au and Na electrodes.[20] Electroconductivity was first discovered in a single-layer device based on poly(paraphenylene vinylene) by Cambridge University researchers in 1990.[6] Inorganic materials (predominantly silicon-based) held the market in semiconducting devices due to the ease and low cost of their design and customization, as well as the possibility of generating films of large area. Early organic semiconducting materials had poor stability, reliability, and performance in comparison to their silicon counterparts. Current LEDS provide emission over the full visible spectrum and have quantum efficiencies comparable to inorganic devices (1-2.5%).[6] A major advantage they hold over inorganic materials is that they form amorphous, glassy films, meaning they can be deposited on rigid or flexible substrates, whereas inorganic materials require crystalline supports. PLED research has commercial roots based on the production of portable

electronics, displays, digital cameras, lighting, automotive systems, and communication systems.

The discovery of electroluminescence paved the way to the creation of organic light-emitting diodes (OLEDs) utilizing small molecules, and then polymers (PLEDs).[5] The basic structure of light-emitting diodes is a single layer of semiconducting polymer between two electrodes, one of which is transparent. Metal contacts apply voltage under a high electric field, causing oxidation of the material at the anode and reduction at the cathode.[21] This leads to the injection of charge carriers (electrons and holes, respectively) into the active layers of the device (Figure 2). The small organic or polymeric material making up the emissive layer must have efficient emission of light and conduction of electricity.

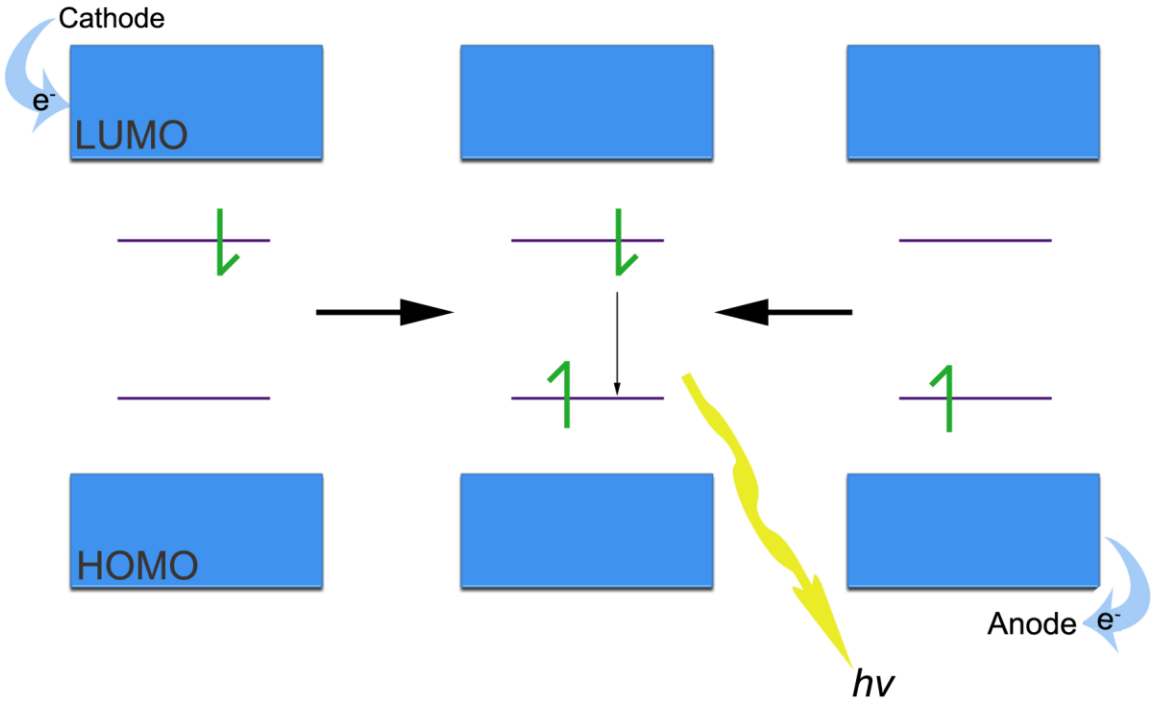

Figure 2. Conduction in a light-emitting diode.

Synthesis and Analysis

Efficiency of semiconductive devices is characterized as internal or external. Internal quantum efficiency is a measure of the number of photons emitted within the material for every electron injected. The statistical maximum is thus 25% because only a quarter of excitons are produced in the singlet state.[21] External quantum efficiency, on the other hand, only measures the photons that have escaped from the device enclosing the material. The external quantum efficiency is further lessened by the number of photons that are reflected by the polymer itself, a parameter that must be considered.[21] For optimum efficiency, the injection rates of electrons from the cathode into the LUMO should equal injection from the anode of holes into the HOMO.[13] Efficiency then can be manipulated not only by the identity of the organic semiconductor, but also by the number of materials in the device.

In single layer devices, the organic layer must perform the three vital tasks: hole and electron transport, and light emission.[13] Because most CPs have low electron affinities and thus have hole-transporting properties, it can be difficult to find a single material that can fulfill these requirements.[2] In multilayer devices, however, efficiency is maximized by having each material carry out a specific function. In two-layer devices, for instance, one polymer may have the task of electron movement (the donor), and the other will be responsible for hole movement (the acceptor). Interestingly, the light emission can still arise from one or both layers.[13] Furthermore, the possibility of excitation from a predominantly donor ground state to a predominantly acceptor excited state allows for fine-tuning of the optical properties of multilayer devices.

Due to the intrinsic tendency of organic semiconductors to photooxidize and degrade upon contact with water, devices in which they are used often must be encapsulated under inert atmosphere.[7] While small molecule conductive materials tend

to be deposited by vacuum evaporation, polymers are more easily electropolymerized or spin-coated from solution onto device electrodes.[13] Successive layers can also be deposited with careful monitoring of solvent compatibility between the layers. The main objectives of continued PLED research is the targeted manipulation of polymeric materials for color tuning, control over the energies of the HOMO and LUMO levels, and the efficiency of light emission.[22]

PHOTOVOLTAIC DEVICES

Theory and Design

Semiconducting polymers can also be used for photovoltaic devices such as solar cells, photodetectors and memory storage devices.[4] The basic process of converting light into an electric current is based on the absorption of a photon into the material, which creates a bound electron-hole pair (exciton). Separation of that pair can result from different mobilities of each carrier in an electric field, each of which must be carried to an external outside circuit, through the electrodes, to form a photovoltage. In order to avoid loss of charges, the energy levels of the electrodes and the semiconducting material must match.[5] The anode must correspond in energy to the level of the HOMO so that it may capture electrons, and the cathode can capture holes by matching the energy level of the LUMO.[5]

The efficiency of photovoltaic devices is thus based on the high charge carrier separation and low recombination, which can be achieved through a large built-in potential difference.[5] The first solar cells were based on hole-conducting CPs solely, and so had low power conversion efficiencies. This led to the use of electron-donor materials (known as "n-type") mixed with electron acceptors ("p-type" materials), which created a potential difference, thereby increasing the efficiency of photovoltaic devices.[12] Solar

energy conversion efficiencies of about 1% were found in the prototypes of devices using these materials. Some devices based on polyfluorene blends have been reported to have external quantum efficiencies in the range of 4-6%.[5]

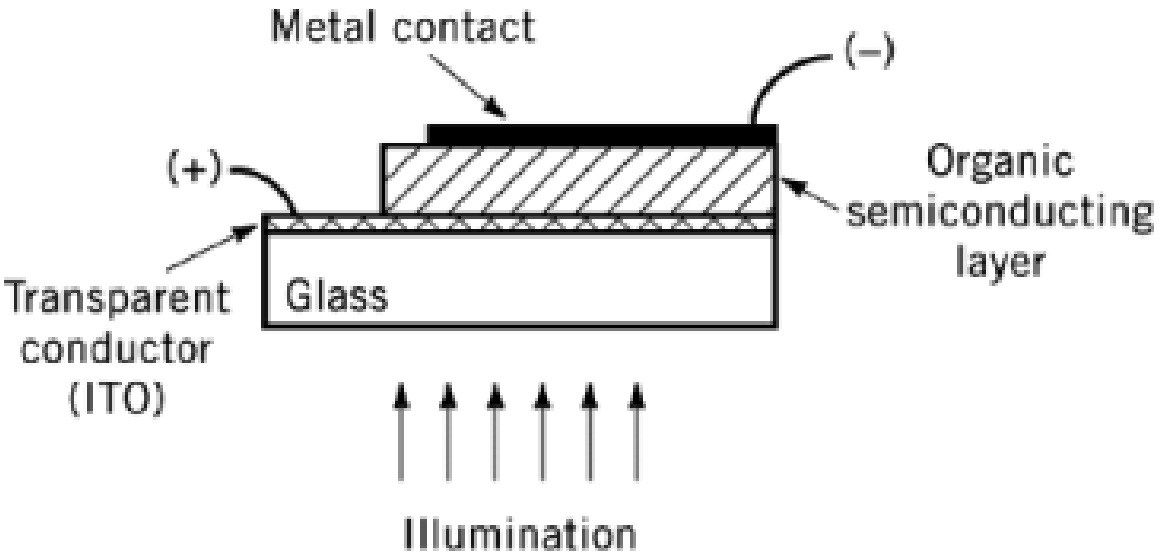

Figure 3. Single-layer photovoltaic device.[4]

Synthesis and Fabrication

In organic semiconducting materials, the positive-negative junction can be made by depositing sequentially n-type and p-type thin films, forcing the movement of carriers to opposite electrodes by the potential across this junction. An increase in exciton mobility is found in rigid, planar structures, and so these are good options for use as dyes in photovoltaic devices. Defects in thin films can trap charges, so films must be made as uniform as possible. Organic materials are more cost effective than inorganic materials to make and purify for use in photovoltaic devices, and they can additionally be deposited in custom-shaped cells. Plastic materials are specifically beneficial for photovoltaic applications requiring a curved surface because they have high mechanical flexibility.[12]

HYBRID MATERIALS

In both photovoltaics and LEDs, the combination of organic semiconducting materials with metals results in a new, promising class of compounds. The structure of hybrid materials can vary from the amorphous to crystalline,[23] revealing the possibility of many applications for these compounds. One prominent example is their use in lithium batteries. Historically, transition metal oxides were used as inorganic slabs sandwiching small organic molecules, then polymers. Currently, the forerunners and most widely studied hybrid materials are those based on silicon networks.[23] In the use of organic and inorganic materials together, the properties of either could be dominant in the device function.

Hybrid materials can be classified by the type of bonding that occurs at the interface of the two materials.[23] Class I materials form ionic or weak interactions, such as ionic, van der Waals, and hydrogen bonds; Class II refers to materials that form covalent or coordinating bonds. The introduction of inorganic compounds into a polymer framework as counterions will result in the formation Class I hybrids, whereas implementation of covalent linkage will form Class II materials.[23] Class II materials encompass many known organometallic chelates that have efficient electron transport and light emission.[13] In the production of Class I materials, the polymer host matrix may be insulating or conductive. Composites of insulating polymers can be used for a number of structural, biomedical or electrical and thermal insulating materials, such as insulation of electrical wires, heat-shrinkable tubing, and compression-resistant foams. While not useful for applications requiring electronic transport properties, these materials can possess flexibility, mechanical strength, optical density, as well as thermal and mechanical properties.

The goal of introducing metal compounds into an organic semiconducting device is the optimization of electrical properties. In the cross-breeding of materials, dissimilar organic and inorganic compounds are combined, often interacting so closely that they function as a single phase. For example, including heavy metal atoms in a framework can result in strong spin-orbit coupling that makes phosphorescence partially allowed.[14] Despite this, it is still possible to tell the difference between metal-centered and ligand-centered behavior. Manufacture of the mixed materials will have a great effect on the desired properties, and can be manipulated. Studies of the interface between materials will often reveal a great deal about the composite.[23] Diminishing particle size yields higher interface/bulk ratio, but particles must not be too small a size, however, because this could blur the difference in the properties of each separate material. With the appropriate approach to synthesis, these organic/inorganic composites can be extremely beneficial for optical and electrical applications.

Chapter 1: Solid-Phase Synthesis of 9,9-Dioctylfluorene-*co*-Benzathiadiazole Oligomers

INTRODUCTION

Polyfluorenes are chemically and photochemically stable materials that can be synthesized in high purity,[22] exhibit strong blue light emission in solution and solid state,[24] and induce stable liquid crystalline properties in polymer films.[25] Despite the rigidly planar structure of the fluorene unit, substitution at the C-9 position does not cause steric effects within the biphenyl structure.[26] In fact, substitution of alkyl side chains at the 9-position creates solubility and stability of the polymer, and can be used to wrap a bulky shell around the polyfluorene main chain.[25] While maintaining a high degree of delocalization, polyfluorene is readily soluble in conventional organic solvents when these substitutions are C_6 or higher. Poly(9,9-dialkylfluorene) exhibits high thermal stability, photoluminescence, hole mobilities, and stability against chemical doping.[25] The absence benzylic hydrogens that can be oxidized in 9,9-dialkylfluorenes means that their main structure and side chains can easily be targeted for specific alterations of physical and chemical properties of the overall polymer.[25]

The utility of polyfluorenes as the sole layer of LEDs, however,[24] is limited by their high band gap energies (about 3.1 eV). The copolymerization of the fluorene monomer with other carefully chosen conjugated units offers the power to tune optical and electronic properties.[27] Efforts made toward reducing or eliminating the anodic and cathodic injection barriers of LED structures[24] have resulted in numerous copolymerizations with polyfluorenes or blends with compatible structures. Because the extent of delocalization in a conductive material can be qualitatively correlated to its emissive colors, copolymers present a good opportunity for the fine-tuning of device

characteristics. A common approach to copolymerization, implemented in the project described below, is through a Suzuki-Miyaura-type process in which an aromatic dibromide unit is reacted with the bisboronate ester of 9,9-dialkylfluorene in the presence of a palladium catalyst.[5]

One such commonly incorporated monomer is 2,1,3-benzothiadiazole (BT), which is often incorporated into low-band-gap materials due in part to the ease of preparing 4,6-dibromo-2,1,3-benzothiadiazole.[28] BT has been combined with electroluminescent dyes and polymers to make efficient green to red OLEDs.[28] Materials containing BT are fluorescent dichromics that align in liquid crystal matrices; they can be used in electrochromic polymers and in the development of biosensors for single-strand DNA and alkaline phosphatase activity.[28] When this electron-deficient compound is attached to the fluorene backbone, the resulting polymer, poly(9,9-dioctylfluorene-*co*-benzothiadiazole) (F8BT), has higher electron affinity (~2.95 eV) and electron-transporting properties (~0.005 $cm^2V^{-1}s^{-1}$) than does poly(9,9-dioctylfluorene). In conjunction with the possibility of color tuning,[29] these properties make it a viable option for many optoelectronic applications.[27]

Despite its highly emissive yellowish-green light,[30] F8BT is often blended with other polymers for use in devices due to its poor hole transport. The electrochemical properties of F8BT have been studied extensively, leading to its use in polymer light emitting diodes (PLEDs), photovoltaic devices, and as the gain medium in distributed feedback lasers.[31] The stiff backbone of F8BT and long alkyl chains produce thermotropic liquid-crystalline phases that align into microscopic monodomains, providing an opportunity for enhancement of charge mobility in these devices.[32] Current efforts on improvisation of F8BT materials lie in the demixing that occurs between

blended polymers during the loss of solvent in deposition, and the resulting wide range of morphologies that can be produced.[33]

Despite this widespread use and the availability of polymeric F8BT from both Cambridge Display Technology and Dow Chemical Company, oligomers of the species are not commercially available. Synthesis of F8BT oligomers by conventional synthetic methods, such as iterative Suzuki-Miyaura couplings, can be an inefficient path due to several inconveniences, such as purification by chromatography at each growth stage and low product yields, especially when aiming to produce oligomers of n=10 and higher. Our project focuses on avoiding this common route in order to improve the synthesis of F8BT oligomers.

One interesting approach researchers have taken for improving the polymerization of other compounds is the use of solid phase synthesis (SPS). With SPS, higher yields can be achieved through numerous conveniences provided by this method. Pioneered by R. B. Merrifield over 40 years ago, this synthetic pathway begins by the attachment of the initial unit of a chain to a resin bead, and repeating successive coupling reactions for sequential attachments. The repeated couplings come at an increased yield in comparison to traditional reactions because the addition of excess reagents guarantees a higher number of attachments.[34] Since the growing polymer is attached to an insoluble solid support, purification at each growth step requires only washes with appropriate solvents, which allows for the recovery of excess reagents through filtration.[35] This process thus is also a more cost-effective approach to oligomer synthesis. After reaching the desired length, the finished oligomers are cleaved from the resin bead and retrieved in pure form.[36]

Originally used for peptide synthesis, SPS has demonstrated its adaptability in recent uses for the synthesis of conjugated homopolymers and block copolymers with

high purity and yield,[37,38] as well as for unique syntheses such as ring-opening metathesis.[39] The fact that high purity can be achieved through this process makes it an especially beneficial approach for the manufacture of semiconductive materials for devices when even low levels of impurities can cause quenching. SPS thus is also a promising avenue for the synthesis of discrete and highly pure F8BT oligomers. The research presented herein describes the development of a synthetic route for F8BT oligomers using SPS, an approach which has previously been unused with this species.

The limited delocalization of CPs has been determined to be 7-13 repeating units, depending on the material,[40] so this project has been undertaken to provide pure samples of n=1-8 F8BT oligomers of well-defined length for single-molecule spectroelectrochemical studies (SMS) focused on the thermodynamics and kinetics of electron transfer.[41] SMS is effective at obtaining more detailed analysis than bulk spectra because the data are less inhomogeneously broadened.[30] This analysis would lead to determining the extent of charge delocalization within the poly(F8BT), since discrete oligomers of sufficient length have been shown to mimic the electron transfer kinetics of the polymer.

EXPERIMENTAL

All chemicals used in the following reactions were obtained through commercial sources and used as received. Unless noted otherwise, all reactions were carried out under inert argon atmosphere in dry glassware. Solvents were dried using a Pure-Solv 400 solvent purification system. ^{1}H and ^{13}C NMR were obtained on a Varian Unity+ 300 and were referenced to the residual solvent peaks. HRMS was carried out on a Thermo Finngan TSQ 700. The syntheses of 2,7-dibromo-9,9-dioctylfluorene (**2**),[42] 2-bromo-7-trimethylsilyl-9,9-dioctylfluorene (**3**),[43] 2-trimethylsilyl-9,9-dioctylfluoren-7-yl-boronic acid (**4a**),[43,44] 2,-(4',4',5'5'-tetramethyl-1',3',2'-dioxaborolan-2'-yl)-7-trimethylsilyl-9,9-

dioctylfluorene (**4b**),[14] 2-trimethylsilyl-9,9-dioctylfluorene-7-yl-trimethyleneboronate (**4c**),[45] and 4,7-dibromobenzo[1,2,5]thiadiazole (**5**)[46,47] were completed following literature procedures. Microwave-assisted reactions were carried out in air in a 20 mL reactor and were performed using a commercial Discover System by CEM. Typical solvent-free reactions were carried out by charging the reactor with 1 equivalent each of compounds **4a** and **5**, 5 mol% catalyst, and 10 equivalents of KF/Al_2O_3 (1:3 w:w).

9, 9-Dioctylfluorene (1)

This procedure was adapted from literature.[48] A mixture of fluorene (20.11 g, 121 mmol), bromooctane (44.5 mL, 230 mmol), KI (2.14 g, 13 mmol), and DMSO (130 mL) was stirred under argon and at room temperature. Powdered KOH (29.57 g, 527 mmol) was slowly added under argon flow, changing the reaction to a gray-green color. The reaction was allowed to stir overnight, poured into water, and then extracted with hexanes. The organic extract was washed with water and dried over $MgSO_4$. After removal of solvents, excess bromooctane was removed by distillation, yielding the product as yellow-orange oil in 76% yield. ^{1}H NMR (300 MHz, $CDCl_3$, ppm) 7.76 (dd, J = 6.8 Hz, 2H), 7.35 (m, 6H), 2.10 (m, 4H), 1.38-1.08 (m, 20H), 0.88 (t, J = 7.2 Hz, 6H), 0.68 (m, 4H). ^{13}C NMR (75 MHz, $CDCl_3$, ppm) 151.0, 141.5, 127.4, 127.1, 123.2, 120.0, 55.4, 40.8, 32.2, 30.5, 29.7, 24.2, 23.0, 14.5.

4-Bromo-7-(9,9-dioctyl-7-trimethylsilanyl-fluoren-2-yl)-benzo[1,2,5]thiadiazole (6)

This compound was synthesized using conventional Suzuki-Miyaura procedure with minor variations. Into a 3-neck flask was mixed compound **4** (1.38 g, 2.37 mmol), compound **5** (0.81 g, 2.76 mmol), aqueous Na_2CO_3 (2.62 g), ethanol (13 mL), and toluene (13 mL). This mixture was sparged with argon for 30 minutes. To this was added $Pd(PPh_3)_4$ (0.0456 g, 0.039 mmol) under argon flow, and then refluxed for 24

hours. The resulting fluorescent solution was extracted with ether, washed with aqueous KOH, brine, and water. The aqueous portion was again extracted with either to remove any remaining organic materials. The organic portion was dried over $MgSO_4$, and solvent was removed *in vacuo*. Purification was moderately successful with column chromatography in 3:1 hexanes: methylene chloride. Product was obtained as fluorescent yellow oil in 34% yield. ^{1}H NMR (300 MHz, $CDCl_3$, ppm) 7.87 (d, J = 9.0 Hz 1H), 7.53 (s, 1H), 2.01 (m, 4H), 1.12 (m, 20H), 0.70 (t, J = 9.0 Hz, 6H), 0.38 (s, 9H).

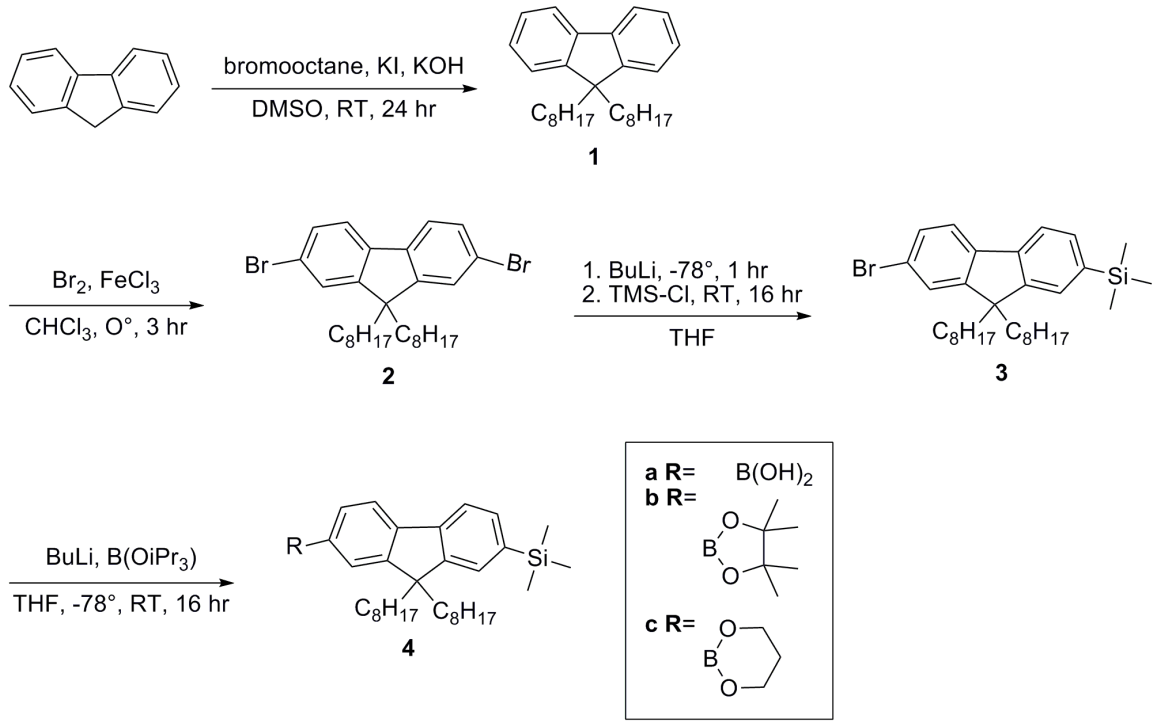

Scheme 1. Synthesis of fluorene monomer.

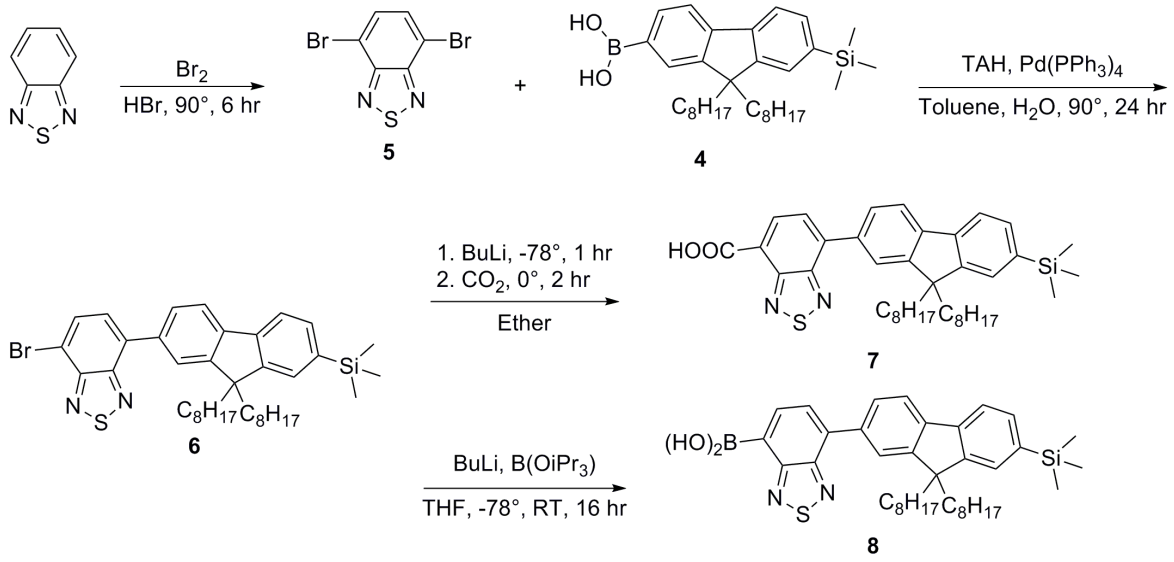

Scheme 2. Coupling of monomers and addition of active groups.

RESULTS/DISCUSSION

The path to synthesizing discrete F8BT oligomers has progressed through the synthesis of the monomer (**6**). The first attempt to attach functional groups to fluorene involved a concerted addition of TMS and boronic acid at the 2 and 7 positions, respectively, but resulted in numerous products with an unclear ^{1}H NMR spectra that proved difficult to purify. The separation of the TMS and boronic acid addition steps facilitated purification at this step and improved yield without any further complications to the outlined procedure. Alternative approaches to this scheme involved attachment of boronic pinacol esters to fluorene (resulting in **4b**, **4c**) in preference to the simple boronic acid. This was carried out in an attempt to increase the yield at this step and in the synthesis of the monomer, compound **6**. The resulting compounds, 2-(9,9-dioctyl-7-trimethylsilanyl-fluoren-2-yl)-4,4,5,5-tetramethyl-[1,3,2] dioxaborolane (**4b**)[14,49] and 2-trimethylsilyl-9,9-dioctylfluorene-7-yl-trimethyleneboronate (**4c**),[45] were also coupled to compound **5** using the same Suzuki-Miyaura coupling conditions as the addition of

compound **4a** (described in entry 7 of Table 1). However, the low yields (34% and 0%, respectively) of this addition, as well as the absence of an increase in coupling yields (24%), led to the rejection of this path.

Entry	Catalyst	Solvent	Aqueous Base	Highest %Yield
1[14,28]	$Pd(PPh_3)_4$	Toluene, Water	Bu_4NOH	2
2[14,28]		Toulene, Water	Bu_4NOH	0[a]
3[50]		Benzene, Water	NaOH	40
4[51]		THF, Water	CsF	0
5[52]		MeOH	KF	7[b]
6[52]		DCM, Water	KF	5[b]
7[52]		N/A	CsF	0[b,c]
8[50]		Toluene, Water	Na_2CO_3	24[d]
9[50]		Toluene, Water	Na_2CO_3	34
10[50]		Toluene, EtOH, Water	Na_2CO_3	45
11[53]	$PdCl_2$-EDTA	MeOH, DCM, Water	K_2CO_3	6[e]
12[53]		MeOH, Water	K_2CO_3	31
13[50]	$PdCl_2(PPh_3)_2$	Ether, Water	N/A	0
14[52]		N/A	KF	35[b,c]
15[52]	$Pd_2(dba)_3$	Toluene, Water	KF	48[b,c]
16[52]		Toluene, Water	KF	0[b,c]

Table 1. Suzuki-Miyaura cross-coupling reaction conditions; a) performed with **4c**, b) used Al_2O_3 as a solid support, c) solvent-free, microwave-assisted synthesis, d) performed with **4b**, e) microwave-assisted synthesis.

The Suzuki-Miyaura coupling process we employed for the synthesis of monomer **6** combines an aqueous/organic solvent mixture, an inorganic base (typically carbonate, bicarbonate, or hydroxide), a palladium catalyst precursor, and a ligand to coordinate to the palladium metal center.[53] This conventional pathway was chosen for our process most often, but microwave-assisted methods, described above, were also employed in our search for higher yielding preparations. The triphenylphosphine ligand we used most often (Scheme 2) is traditionally used for these coupling reactions, but electron-rich bulky phosphines, phosphine oxides, and phosphine-based palladacycles can also be used.[53] For example, Korolev and Bumagin reported a 62-96% coupling yield using $PdCl_2$-EDTA for numerous aryl halides and arylboronic acids of varying composition.[53] While our use of this catalyst gave much lower yields, 6% and 31% for microwave and conventional reactions (entries 11 and 12, Table 1), respectively, they are based on conditions lacking Bu_4NBr. We replaced this compound with methanol for the inclusion of water-insoluble compound **5**; this modification resulted in a less efficient process with a difficult purification. However, Bu_4NBr did not fulfill its phase-transfer properties when included in the traditional Suzuki-Miyaura conditions (entries 1 and 2), which resulted in a 2% yield.

Other synthetic attempts with catalysis by $Pd(PPh_3)_4$ (entries 3-10) varied in their specific reagents and solvents, and were prepared in the conventional manner. Yields ranged from zero conversion to 45%, the latter of which occurred after the accidental evaporation of the solvent during reflux. With careful monitoring, this reaction (run under traditional conditions with the addition of ethanol for inclusion of compound **5**,

entry 11) could be the optimum for synthesis of our copolymers. Also promising are the reaction conditions with the highest overall yield (48% entry 15), which was obtained when searching for other reaction conditions for improving yield and limiting the number of side products.

Using $Pd_2(dba)_3$, the highest yield was possible with the use of KF as a base, and Al_2O_3 as a solid support holding the catalyst and salts formed in the course of the microwave-assisted reaction.[52] The pioneers of this approach effectively coupled phenyl iodides with phenylboronic acids and recovered the product by simple filtration with non-polar solvents, separating them from the solid supports.[52] The combination of reagents and solvents they used did not alone serve to raise the yield of our coupling reaction, however, as can be seen in the other attempts utilizing different catalysts (entries 5, 6, 14, and 16). It is likely that the catalyst $Pd_2(dba)_3$, in combination with a solvent-free microwave-assisted setup, is a worthwhile approach for our coupling of 2-trimethylsilyl-9,9-dioctylfluoren-7-yl-boronic acid (**4a**) and 4, 7-dibromobenzo[1,2,5]thiadiazole (**5**).

The goal of limiting side products was particularly important for revision of our pathway given that the synthesis of **6** typically resulted in 8-10 fluorescent products on a TLC run in 3:1 hexanes-methylene chloride, none of which were starting materials. While improved chromatographic technique aided in the isolation of the desired product from byproducts of similar R_f values, an overlapping compound on the TLC of this sample has proved difficult to remove. Similar in all our coupling attempts was the further complication in purification of a thick emulsion during extraction, which required many washes to remove as much product as possible. Attempts to isolate compound **6** through recrystallization from different solvents were unsuccessful. While these setbacks in purification likely contributed to our low yields, we hypothesize that they are minor compared to having less-than-ideal reaction conditions.

The synthesis of compound **7** was attempted numerous times through the use of BuLi[54] (Scheme 2) with zero conversion, and twice as a Grignard reaction,[38] also without success. The absence of product was confirmed by a ^{13}C NMR spectrum that lacks a COOH carbon peak (Figure 4) and an IR without a broad OH band (Figure 5). To test for the presence of a carboxylic acid group, a small sample was mixed with water, and to this was added sodium bicarbonate; the lack of fizzing and/or white precipitate indicated COOH was not present. A second test called for the dissolution of a small amount of crude product into dilute NaOH(aq); this test was also failed. Both procedures resulted only in starting material, offering no information about possible errors in the reaction.

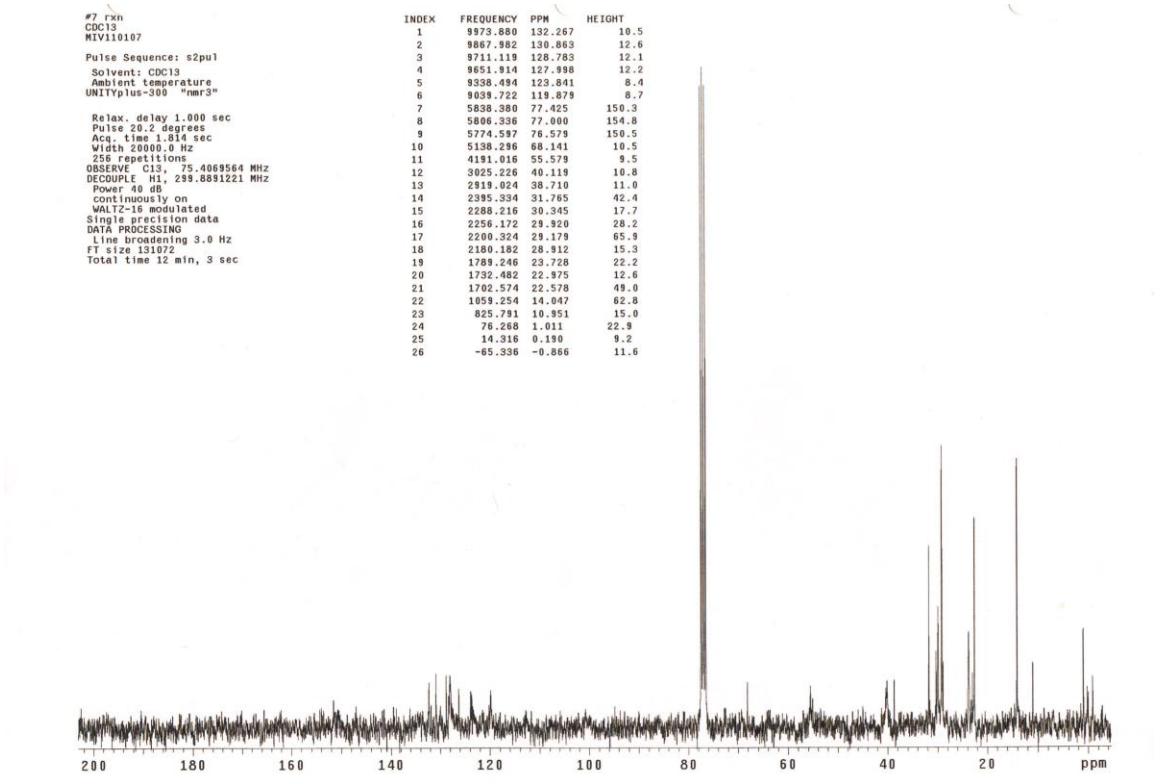

Figure 4. ^{13}C NMR of the reaction product when attempting to make compound **7**.

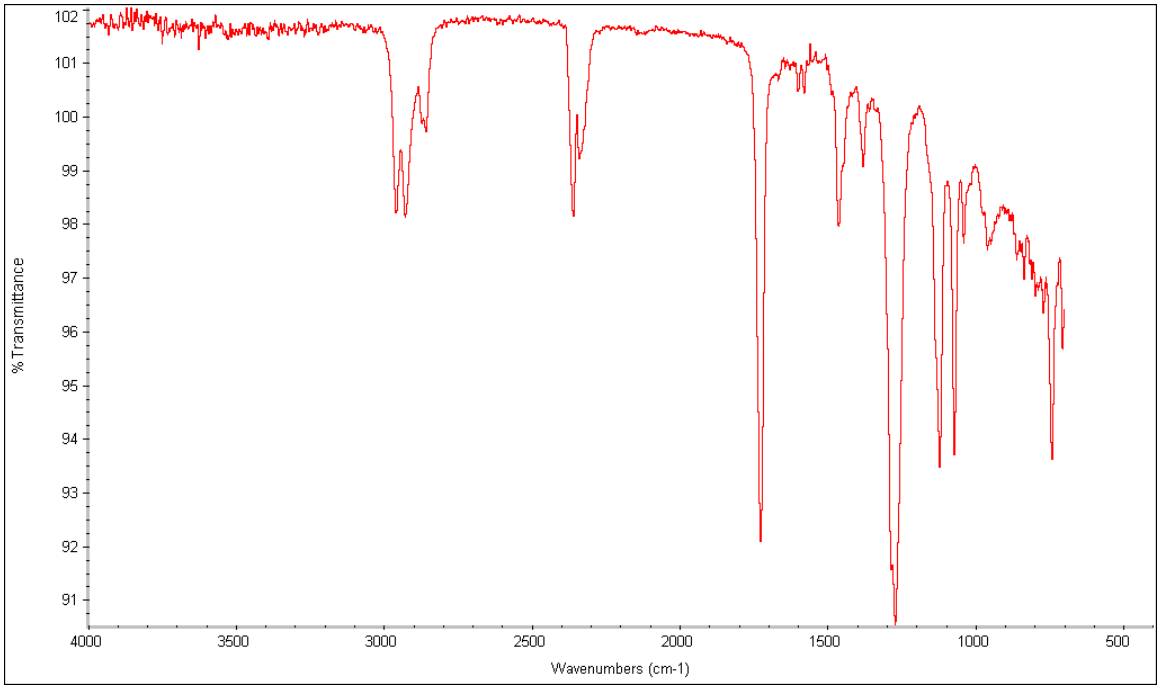

Figure 5. IR of the reaction product when attempting to make compound **7**.

FUTURE DIRECTIONS

Successful addition of the carboxylic acid for the preparation of compound **7** would lead to attachment to a Merrifield resin bead,[55] and then substitution of the bromine with a boronic acid group for monomer coupling. Scheme 3 illustrates the continuation of the synthetic protocol after addition to the solid support. The conversion of the TMS group of the attached monomer to create compound **10** can also be performed through the use of ICl, CH_2Cl_2, at 25 °C[14] or with $Pd_2(dba)_3$, PPh_3, and CuI in 1:4 Et_2NH/THF.[37] The last unit added to a growing portion (**8**) will contain only a boronic acid in the 2-position. Once the oligomer of desired length is produced (compound **12**, Scheme 4), the chain will be cleaved from the bead to produce a terminal ester (**14**).[55]

The methyl group of this ester will be cleaved to make compound **15** and the subsequent removal of the carboxylic acid group will be achieved through a reaction with copper.[55]

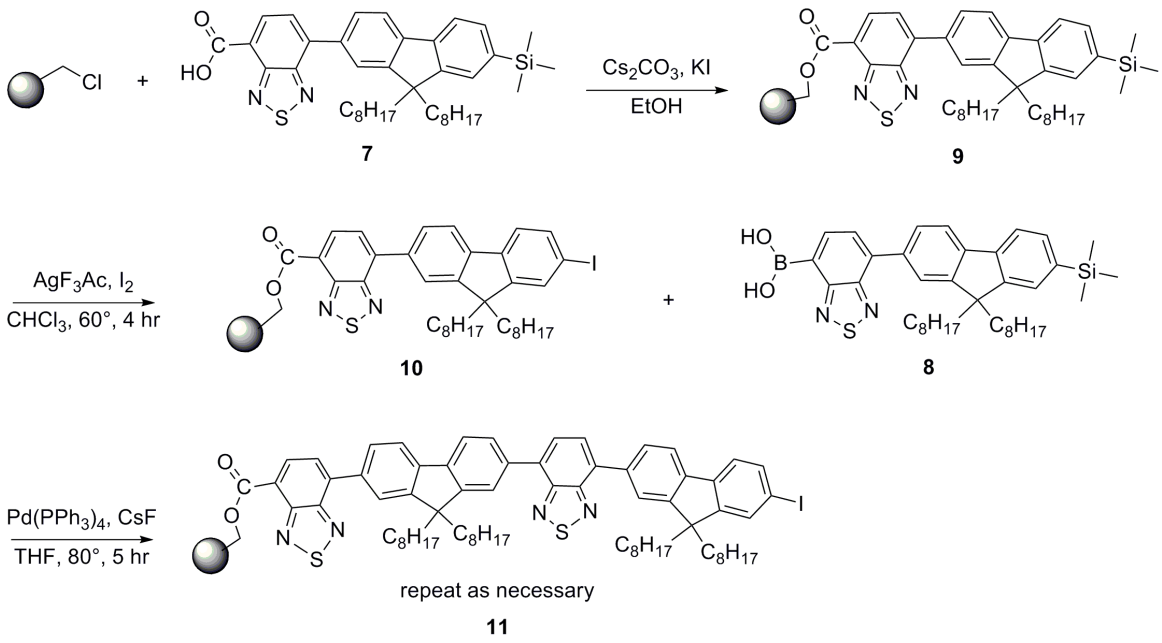

Scheme 3. F8BT oligomer solid phase synthesis (SPS).

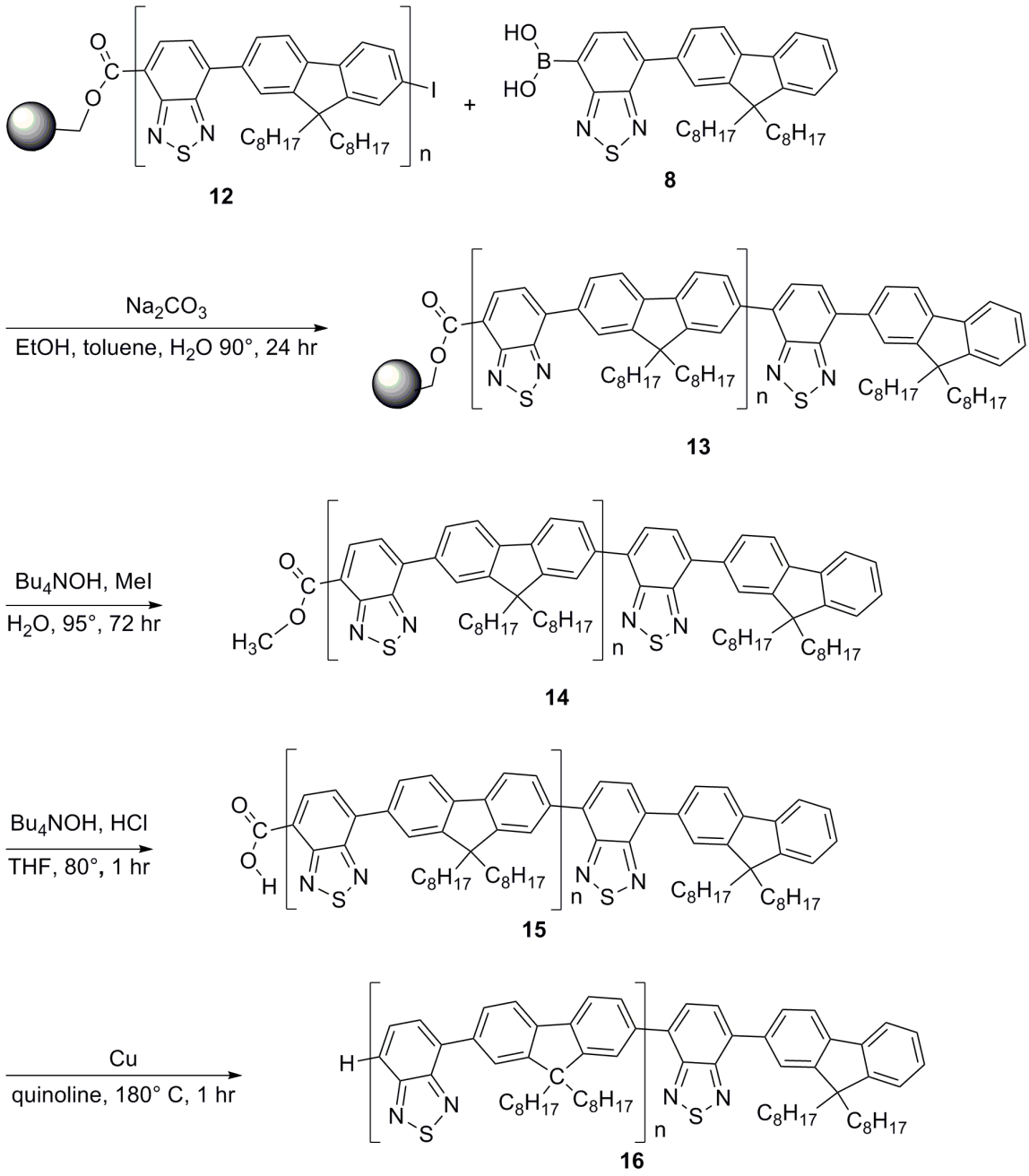

Scheme 4. Removal of F8BT oligomer from Merrifield resin bead.

Chapter 2: Synthesis of Alkylated Sexithiophene Series

INTRODUCTION

Polythiophenes (PTP) have electrical, electrochemical and optical properties that can be useful in various applications.[56] The electronic structure of the polymer is based on the connection between the two sulphur π electrons in each monomer and the four π electrons of the carbon, which forms a local six-electron system.[9] In doping PTP, the injected carriers are delocalized over many carbon atoms, leading to a large effective mass for conductivity.[9] When these localized regions begin to overlap, high conductivity is obtained through a process known as a bipolaron mechanism.[3] This is a combination of charge movement along the polymer chain and the charge-hopping mechanism between polymer chains. The activation barrier that must be overcome for this mechanism to occur is usually small once the overlap occurs, and the conductivity is essentially metallic when the barrier approaches zero.[9] The electrons of PTP have been found to be delocalized over 5-7 thiophene units.[9]

CPs naturally tend to form stacks because of their π-delocalization,[17] and polythiophene is no different. In alkyl-substituted polythiophenes, the attached chains act as spacers between induced polymer layers (lamella). The lamella then stack in a regular array, one above another, to form three-dimensional structures (Figure 6Figure 6).[57] This packing optimizes conduction between stacks by allowing electron orbital overlap between adjacent polymer chains. In fact, the large carrier mobility found to occur perpendicular to these thiophene planes composes the highest conductivity in the polymer.[9] This is due to the large overlapping of π_z orbitals between chains, despite the fact that the orbitals that are adjacent on carbon atoms along each chain couple at a larger magnitude than the end-on orbitals.[9]

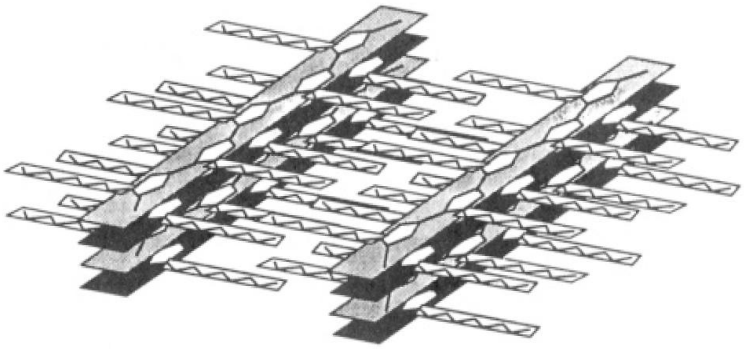

Figure 6. Lamellar packing of poly(alkylthiophenes).[57]

Synthesizing thiophenes with alkyl substituents has led to a large advance in materials research because of the processability, air stability, and low band gap energies of their resulting polymers. The most common substituents are $C_{6\text{-}12}$ chains at the 3-carbon position, utilized to make soluble the otherwise insoluble polymer.[58] This property allows for poly(3-alkylthiophenes) (P3ATs) to be studied in solution or as cast films,[57] making them workable materials for electrical devices. Substitution also creates the possibility of different polymer chain conformations, which in turn alters the macroscopic structure of the bulk polymer. It has been shown that substituent modification is an effective and practical way to tune optical properties,[59] and even improve conductivity[18] in CP materials.

The stereoregularity of P3ATs can exemplify this connection. The numerous arrangements that can result from polymerization are classified into a system based on the arrangement of two coupled monomers that are linked at the 2- and 5-positions. The configuration of each unit is labeled “head” or “tail” in relation to the other monomer. If the 3-substituent of the first monomer is at the 2-position relative to the second, this is

termed as a head configuration, whereas a connection of a monomer through its 5 position implies the substituent is in the tail configuration.[60] Between two units, couplings may be 2, 5' (head-tail, HT), 2, 2' (head-head, HH), or 5, 5' (tail-tail, TT). These three possible conformations of two coupled monomers translates into four forms of coupling in a polymer chain of poly(3-alkylthiophenes): HT-HT, TT-HT, HT-HH, and TT-HH.[3] Because research and development efforts are aimed at device optimization, structures with such irregularity pose a challenge for accurately characterizing and customizing materials.

Knowing and understanding molecular organization, backbone conformation, and molecular packing are powerful means for understanding the electronic properties of polythiophenes.[16] In regioregular P3AT, which is defined as having a majority of side-chains arranged in the head-to-tail conformation, the charge-carrier mobility is at least two orders of magnitude greater than that of its regiorandom counterpart.[61] This is due to the HT conformation (Figure 7A) being of lower energy than the HH (Figure 7B) configuration.[57] The regiorandom polymer, with fewer side-chains in HT arrangement, contains thiophene rings forced out of coplanarity and conjugation with each other. The size of the bandgap in poly(3-alkylthiophenes) increases with the size of this torsion angle between thiophene rings. This alteration creates microstructural irregularity responsible for the decreased level of conductivity in regiorandom P3ATs. Current efforts aim at ensuring the isolated synthesis of regioregular P3ATs for this reason.

This variance of conductivity is also dependant on the specific structure of the substituent. The length of attached alkyl chains, for instance, has been found to be the most important factor in the distance of co-facial solid packing of the polymer,[57] which in turn directly affects orbital overlap. Such structural alterations can be more pronounced in structures with larger alkyl substituents. *Ab intio* calculations of poly(3-

hexylthiophene) and poly(3-cyclohexyl-thiophenes),[59] for example, were used to calculate torsion potential curves in these compounds. The polymer optical properties were then explained in relation to each substituent.[59]

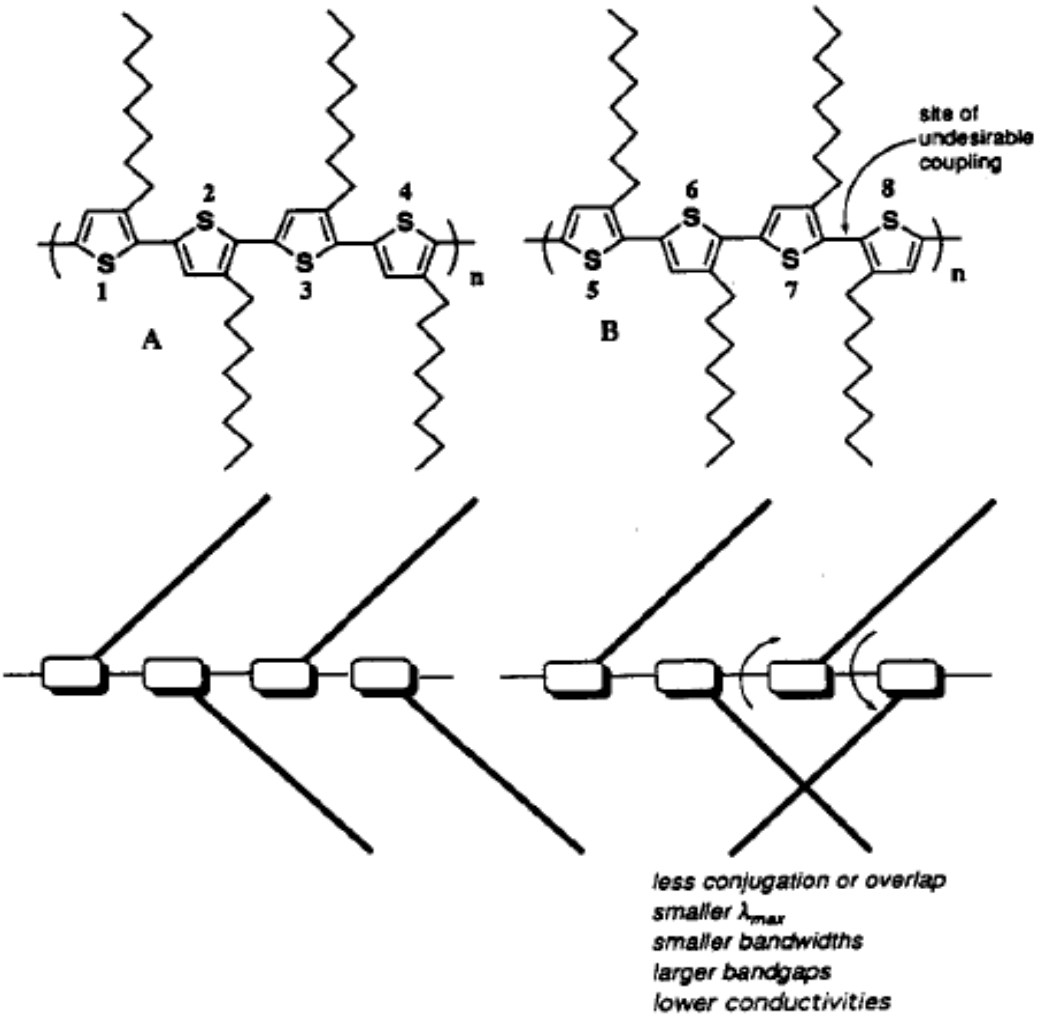

Figure 7. Microstructural irregularity in poly(3-alkylthiophene).[3]

This direct correlation between substituent effects and conductivity make the selection of substituents an important decision in preparing materials for electrical

devices. Because the microscopic and macroscopic structures of a conjugated polymer define its electrical and optical properties,[3] customization of polythiophenes in this way will ensure an effective approach to material design. The project outlined below is thus focused on modifying the conductive properties of PTPs by interchanging substituents on the thiophene ring. Synthesis was focused on oligothiophenes with substituents at the 3- and 4-positions, however, to avoid the unnecessary complication of stereoregularity. Oligothiophenes were chosen over polythiophene in the interest of avoiding barriers to accurate analysis such as distribution of molecular weights, coexistence of amorphous and crystalline domains, as well as structural and chemical defects.[56] Thus through a systematic approach, synthesis of the oligomers could more likely produce isomerically pure products[62] than could polymerization of polythiophenes with asymmetric substitution.

The study and use of oligothiophenes in various applications is widespread. Oligothiophenes are looked at favorably for use as semiconductors in electronic and optoelectronic devices, and sexithiophene specifically was the basis for the first all-organic transistor.[18] While electronic devices comprise the main application of oligothiophenes, it has also been found that some bi- and terthiophene derivatives have biological implications through such characteristics as phototoxicity, or antibiotic and antiviral properties in the presence of UVA light.[63] The use of oligothiophenes in electronic applications is limited to longer structures because most of these short oligothiophenes do not have the appropriate electronic properties needed for device manufacturing. Conjugated oligothiophenes have been employed as the active materials in numerous devices, including molecular electronics,[64] thin film transistors, photovoltaic solar cells, light-emitting diodes, spatial light modulators, electro-optical modulators, photochromic switches and laser microcavities.[63]

Well-defined oligothiophenes posses a high degree of molecular and crystalline ordering relative to the parent polymers,[63] and that advantage extends to the thin films of both materials.[18] They retain the magnitude of electrical conductivity found in full polymers[3] and have good charge mobility, efficient fluorescence, and high chemical stability.[52] The structure of unsubstituted oligothiophenes reflects the parallel fashion of the parent polymer. However, arrangement of the molecular planes side-by-side molecules form angles of 40-60° between them,[63] creating a "herringbone" pattern of crystallization (Figure 8). This structure is also typical of other aromatic hydrocarbons such as para-oligophenylenes and acenes. Herringbone packing is mainly due to repulsion between π orbitals of neighboring molecules and can be changed to a π-stacking conformation through substitution or doping. Substitution on the thiophene ring can create strong enough intermolecular interactions to overcome the π-π repulsion.

It has been proven that quantum yield and lifetime increase with an increase in thiophene units (*n*) from *n*=2-5, but become constant at *n*=5-7.[18] Our focus on varying sexithiophene structures is supported by this evidence as well as findings of soluble sexithiophenes to be nearly planar in the solid state, self-assembled in parallel layers, and capable of high charge transport properties.[52] The project outlined below aims to improve thiophene compounds for the fabrication of energy materials by altering sexithiophene packing structures after deposition on device electrodes and other substrates (**Error! Reference source not found.**). Through the synthesis and characterization of various tetra-substituted-sexithiophenes (compound **22**), we hope to expand what is known about the conductivity within and between sexithiophene chains. Furthermore, we hope to characterize the interaction of these compounds with different substrates in order to determine their charge energy and transfer at the interfaces of electronic devices. The proposed products of our synthesis would later be evaluated for

structure/property correlations, such as through the prediction of equilibrium torsion angles and energy barriers by conformational analysis in order to reveal more about the substituent effects in thiophene materials.[59]

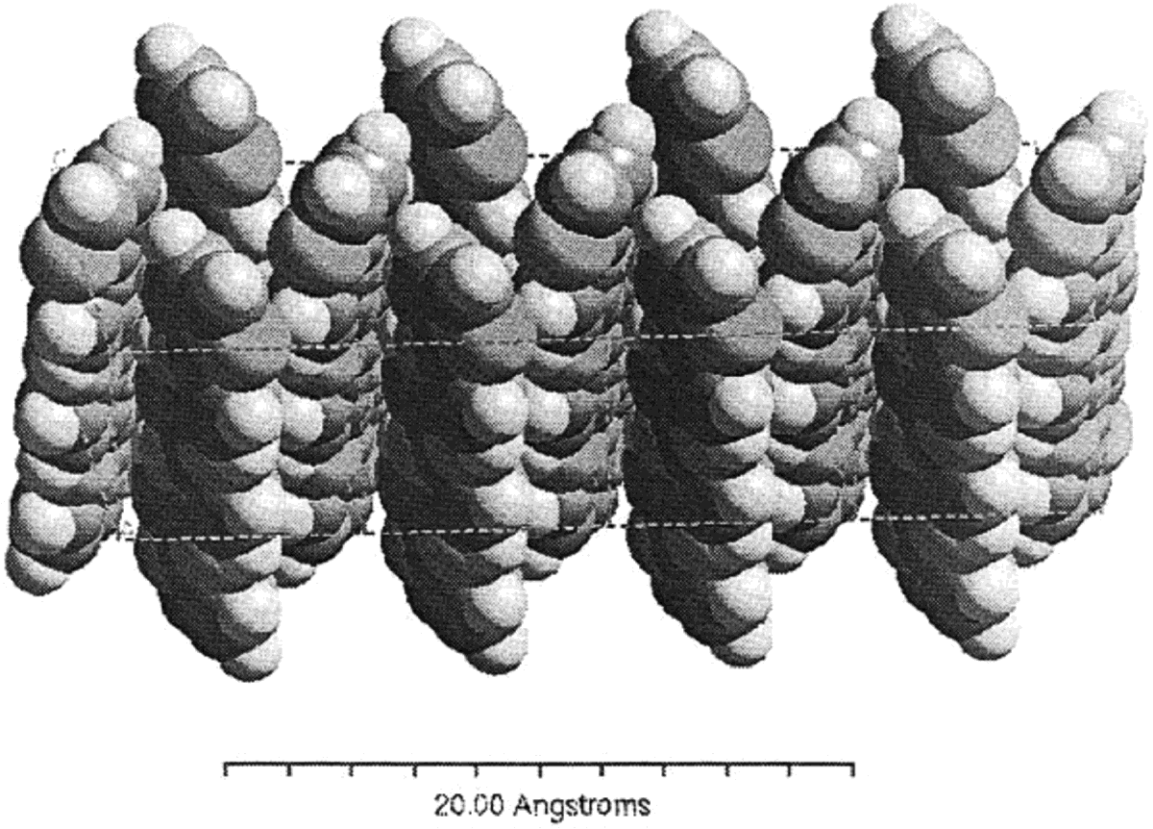

Figure 8. Lattice packing of unsubstituted sexithiophene.[65]

Resulting studies of the target molecules will also look at different methods of processing and deposition that is possible with the proposed substitutents. One tactic is orienting the sheet-like organization of the polymer backbone so that the thiophene ring plane is orthogonal to the plane of the substrate.[11] Surface treatment can have a large effect on this orientation. For example, structure analysis methods on poly(2,5-bis(3-

dodecylthiophene-2-yl)thieno[3,2-b]thiophenes) (pBTTT) (**Error! Reference source not found.**) have demonstrated a great dependence of morphology, molecular orientation, and charge carrier mobility on substrate chemistry.[8] This CP provides a directly measurable substrate effect due to its large thin film domains and orientation. Kline *et al.* treated silicon oxide surfaces with hydrophobic agents to reveal a likely chemical, and not topographical, involvement of the substrate with the deposited pBTTT.[8] The proposed "pinning" of molecules to the surface that improves charge transport is increased by the large size and orientation of pBTTT crystals.

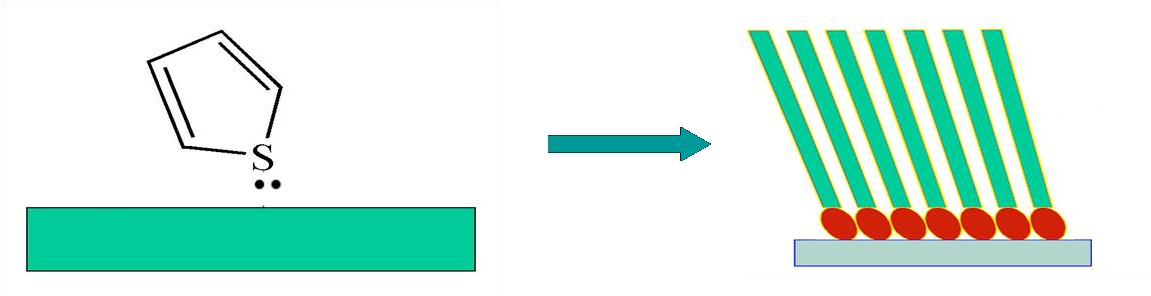

Figure 9. General adsorption and surface packing of polythiophenes.

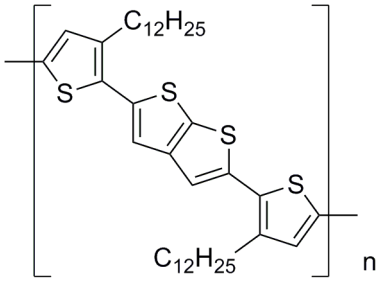

Figure 10. Poly(2,5-bis(3-dodecylthiophene-2-yl)thieno[3,2-b]thiophenes) (pBTTT)

The systematic approach taken to alter the crystal packing of tetra-substituted-sexithiophenes involves the use of different R substituents (illustrated in

Table 2) on compound **22**. While polythiophenes are often made through electropolymerization or chemical oxidation of the monomer, oligothiophenes can be made by synthetically linking individual units. Using defined building blocks leads to a well-defined structure,[66] which is a necessity in regard to full characterization. The preparation of our varied sexithiophenes always begins with substitution on a thiophene ring. This becomes the center unit in a terthiophene moiety after the coupling of single thiophene rings on either side. Two of these terthiophenes are then coupled together (Scheme 6) to produce the final sexithiophene.

Scheme 5 outlines the only asymmetric substitution attempted in this project. The structure chosen to attach to the central thiophene ring is one based on the field of polymer structure modification through the use of liquid crystals (LCs). The unique properties of LCs ensure that polymers containing these moieties will have significant alterations to overall structure. For instance, LCs respond to even weak electronic and magnetic fields with significant structural changes.[67] They are anisotropic in that they point along a special direction most of the time, and response to external fields will vary depending on whether or not the field is applied along that direction.[67] With induced or permanent dipoles along or across the long axis of the molecule, liquid crystals rotate until their positive and negative regions aligned up with the electric field.[67] This change of orientation is a property that makes them like liquids.[67] Conversely, they also maintain the solid property of orientational order among the molecules.[67]

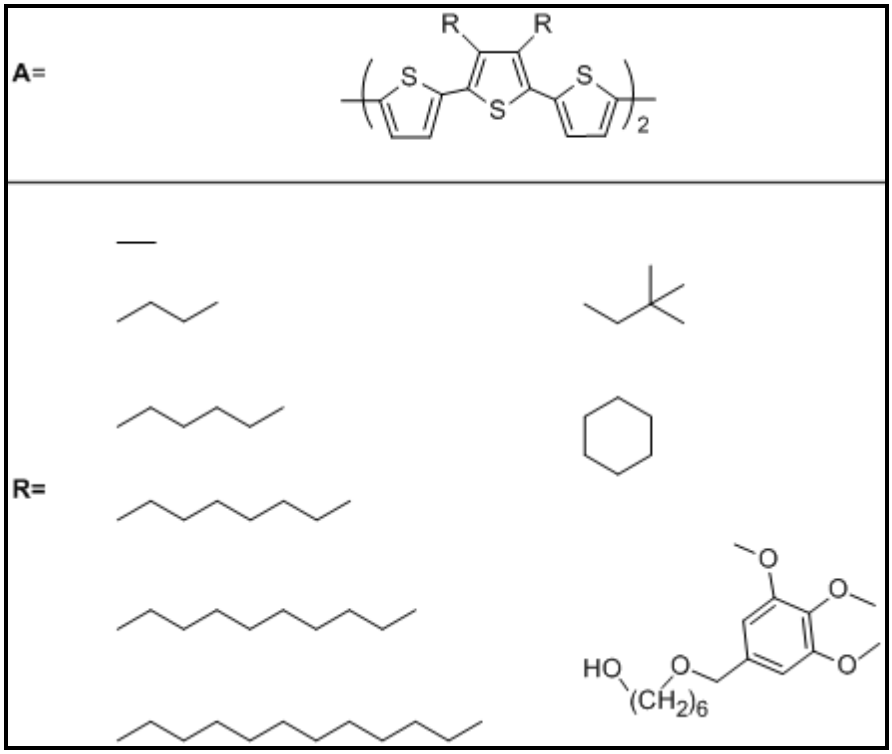

Table 2. Our proposed library of sexithiophene compounds.

These liquid and solid-like properties assured our aims of altering the expected sexithiophene morphology while creating the possibility of achieving high charge mobility by forcing rapid transfer between the overlap of π orbitals.[13] The pendant group utilized in the Scheme 5 synthetic pathway was inspired by the initially targeted molecules of this field (**Error! Reference source not found.**). Production of LCs based on two main approaches: a) construction of cores followed by synthesis or modification of the pendant chains, or b) the attachment of chains to a preformed core.[68] The most extensively studied liquid crystals are calamatic with the formula R'-A-L-B-L-C-L-C-R" where R' and R" are terminal groups, A-D are ring systems, and L are linking units.[68] The stability of these LCs is determined by the terminal groups based on the spectrum: $CN>OCH_3>NO_2>Cl>CH_3>I>CF_3>H$.[68] For interactions between fragments, alkoxy

substituents provide better results than alkyl substituents with phenyl groups.[68] The target molecule (**18**) thus incorporates a terminal trimethoxy substituted phenyl group.

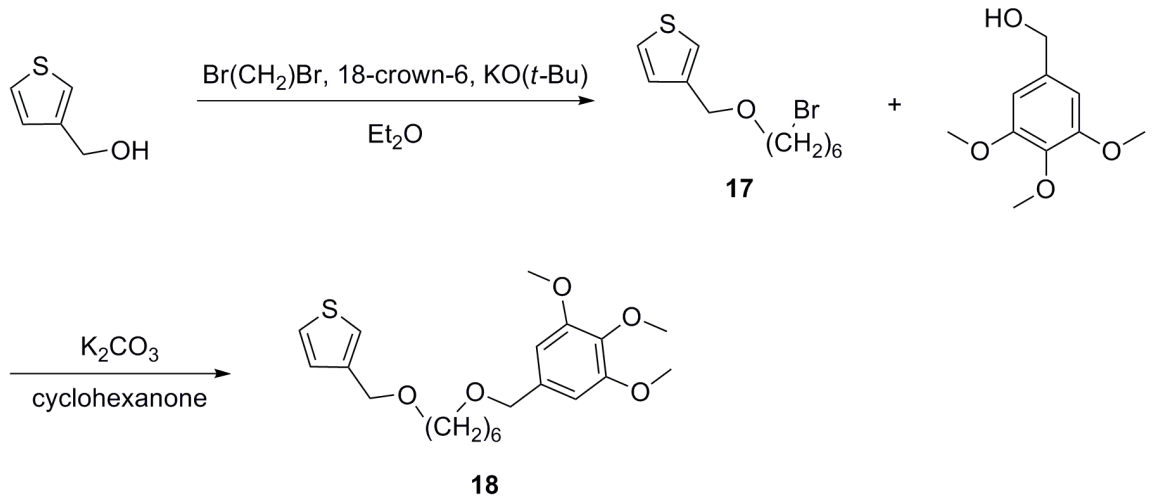

Scheme 5. Pendant group substitution on thiophene.

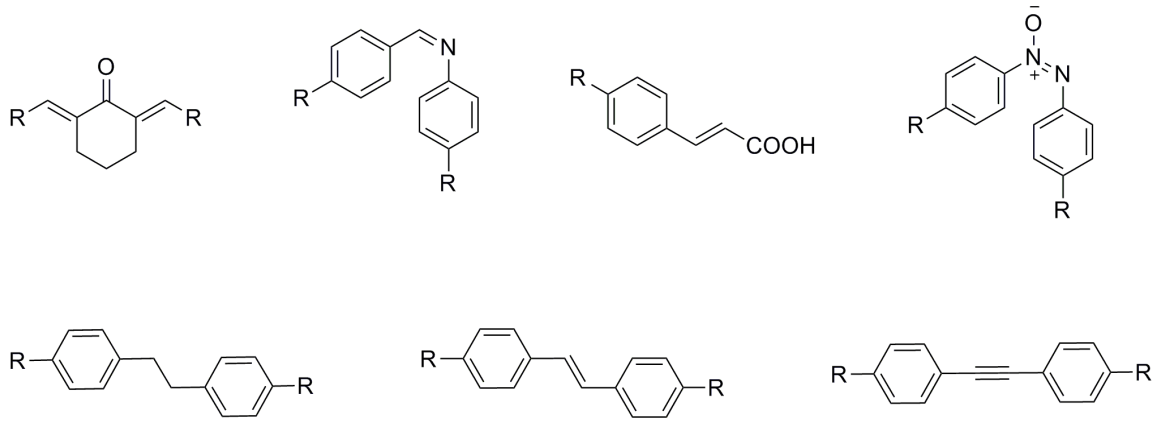

Figure 11. Early target molecules for liquid crystal synthesis.

The goal of substituting straight alkyl chains at the 3- and 4-carbon positions on our target sexithiophene (**22,** Scheme 6) was based on the successful preparation of the R=C_4H_9 and C_6H_{13}, and C_8H_{17}[64,69] by other research groups. The isolated basic structural and conductive analyses following the synthesis of these compounds provide great

insight into our proposed study of a series of substituents on sexithiophene. For example, the crystal and molecular structures of 4’’’’-tetrabutyl-2,2’:5’,2’’: 5’’,2’’’: 5’’’,2’’’’:5’’’’,2’’’’’-sexithiophene (TBST), were elucidated by Liao, *et al.* in 1994,[16] revealing an average dihedral angle of 12.6° between adjacent rings and a mixture of two main conformations. The terminal thiophene rings of TBST show a *syn*-conformation with respect to their neighbors (**Error! Reference source not found.**a) in up to 40% of molecules in a unit cell, whereas an all-*anti* conformation (**Error! Reference source not found.**b) is present in about 60%. The majority *anti*-confirmation of the S-atoms adjacent to alkyl groups minimizes steric crowding.

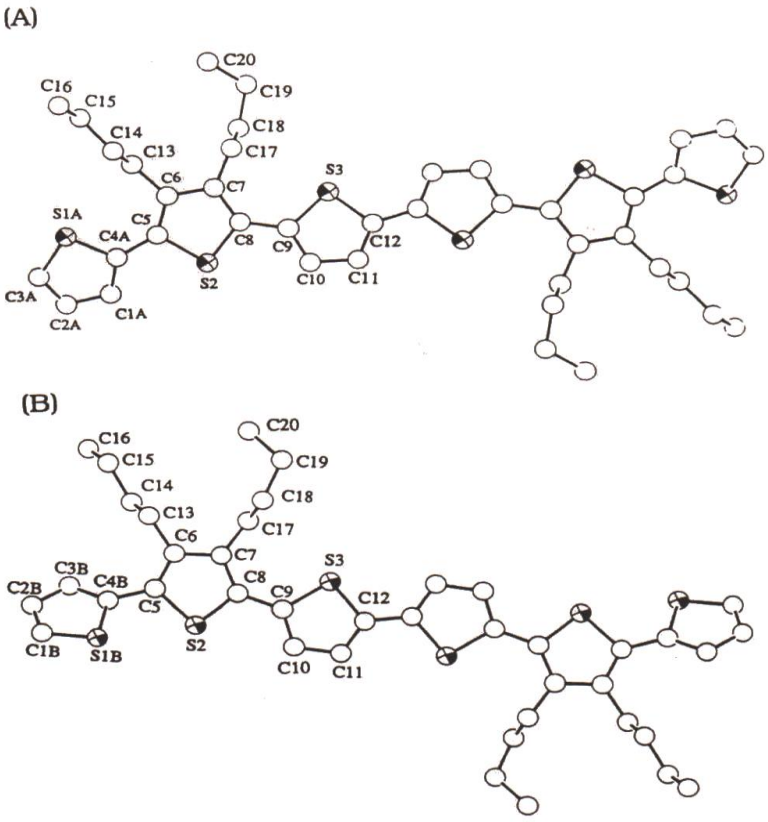

Figure 12. Molecular structure of 3',3"",4',4""-tetrabutylsexithiophene. a) All-*anti* conformation, occurring in 60% occupancy of the crystal. b) Rotational isomer with terminal rings in the *syn* conformation.[16]

These researchers proposed that the minor *syn*-conformation is also present in the full polymer, in which it causes rotational defects. The resulting kinks and bends can interrupt the conjugation of the backbone and thus decrease charge carrier mobilities. The crystal structure of TBST also revealed a deviation in coplanarity by the terminal thiophene rings of up to 19° for both *anti* and *syn* arranged rings. While it is not proven to persist after doping, this out-of-plane conformation could affect charge transport from chain-end to chain-end, thereby decreasing carrier mobility. We hope that some of the analysis arising from our series of sexithiophenes with alkyl chains ranging from C_2 to C_{12} can reveal ideal structures for avoiding these concerns, or at the very least, elucidate further the relationship between specific alkyl substitutions and carrier mobility.

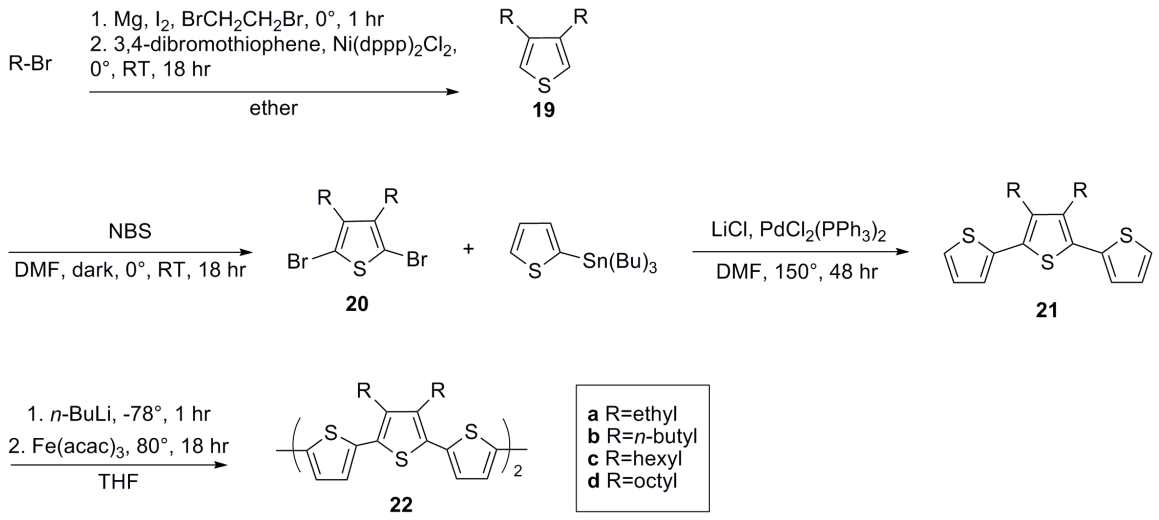

Scheme 6. General Synthesis of 3',4',3''', 4''''-Tetraalkyl-2,2':5',2'': 5'',2''': 5''',2'''':5'''',2'''''-sexithiophene dervatives.

The use of bulky alkyl substitution to produce compound **26** as the center thiophene ring in the creation of a sexithiophene was also approached as a means of

altering oligothiophene thin film morphology. It has been found that branched alkyl groups can directly affect the solid-state physical properties and morphologies of the resins in which the branches occur.[70] In terms of microstructure, the attachment of a neopentyl group would create a sterically overcrowded thiophene ring with high internal strain.[71] Scheme 7 outlines the published preparation that was begun for the attachment of this group and was considered for use with cyclohexyl groups. The method was pioneered by Nakayama, *et al*. for the attachment of congested thiophenes and/or angle-strained thiophenes.[71-75] Of particular interest for our project was their use of neopentyl, tert-butyl, and 1-adamantyl groups on thiophene rings. The synthesis begins with the intramolecular reductive coupling of 3-thiapentane-1,5-diones to form thiolane-3,4 diols or 2,5-dihydrothiophenes.[72] These are converted to the final product in high yields by dehydration and dehydrogenation, respectively.

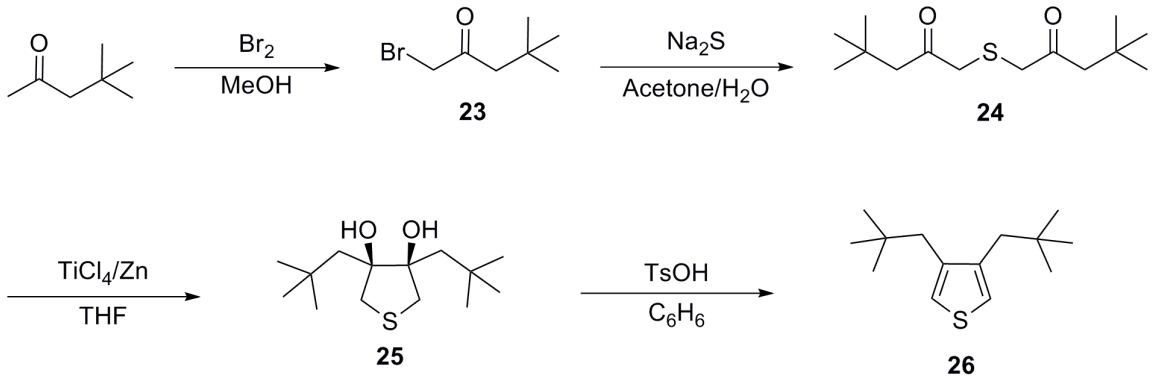

Scheme 7. Bulky alkyl substitution on thiophene.

EXPERIMENTAL

All chemicals used in the following reactions were obtained through commercial sources and used as received. Unless noted otherwise, all reactions were carried out

under inert argon atmosphere in dry glassware. Solvents were dried using a Pure-Solv 400 solvent purification system. ^{1}H and ^{13}C NMR were obtained on a Varian Unity+ 300 and were referenced to the residual solvent peaks. HRMS was carried out on a Thermo Finngan TSQ 700. Literature methods were followed for the preparation of 3-(6-bromohexyloxy)methylthiophene (**17**),[76] 3,4-dibutylthiophene (**19b**),[77] 2,5-dibromo-3,4-diethylthiophene (**20a**),[78] 2,5-dibromo-3,4-dibutylthiophene (**20b**),[62,79] 2,5-dibromo-3,4-dihexylthiophene (**20c**),[80] 2,5-dibromo-3,4-dioctylthiophene (**20d**),[81] 3',4',3''', 4''''-tetrabutyl-2,2':5',2'': 5'',2''': 5''',2'''':5'''',2''''':-sexithiophene (**22b**) and 3',4',3''', 4''''-tetraoctyl-2,2':5',2'': 5'',2''': 5''',2'''':5'''',2''''':-sexithiophene (**22d**),[69] bromo-methyl neopentyl ketone (**23**)[73] and 1,5-dineopentyl-3-thiapentane-1,5-dione (**24**).[72]

General Procedure for the Addition of Alkyl Chains to Thiophene (14)

The following compounds were synthesized by the general Grignard reaction procedure described here, with specific alterations noted with the appropriate structure. Magnesium turnings (1 eq) were crushed and immediately placed in a dry 3-neck flask under inert argon atmosphere. Dry ether was added, followed by sufficient iodine for color change, and 1-2 drops of dibromoethane. A few drops of bromoalkane were added, and stirring was continued until the mixture lost all orange color and turned gray. The flask was set on ice and the remaining amount of bromoalkane (1.2 eq) was added dropwise to maintain a gentle reflux. After stirring for 30 minutes, the solution was transferred to another dry 3-neck flask containing (5% mol eq) Nidppp in ether. This flask was also set on ice and 3,4-dibromothiophene (1 eq) was added dropwise. The mixture was cooled to RT, and then heated to reflux for 18 hours. After cooling to RT, the mixture was hydrolyzed by dropwise addition of 10% HCl solution at 0°C. The organic portion was extracted by ether and washed with water three times. The extracts

were combined and dried over MgSO4, evaporated, and purified by silica column chromatography in hexanes.

3,4-Diethylthiophene (19a)

Prepared according to general procedure in THF.[82] Colorless oil was obtained in 48% yield. ^{1}H NMR (300 MHz, $CDCl_3$, ppm) 6.77 (s, 2H), 2.43 (d, J = 6.9 Hz, 4H), 1.14 (t, J = 6.9 Hz, 6H). ^{13}C NMR (75 MHz, $CDCl_3$, ppm) 143.2, 119.4, 21.8, 13.6. MS (CI+) *m/z* calculated for $C_8H_{12}S$ $(M + H)^+$ 141.25, observed 141.

3,4-Dihexylthiophene (19c)

Prepared according to general procedure. Colorless oil was obtained in 42% yield. ^{1}H NMR (300 MHz, $CDCl_3$, ppm) 6.88 (s, 2H), 2.50 (t, J = 6.9 Hz, 4H) 1.63 (m, 4H), 1.34 (m, 12H), 0.90 (s, 6H). ^{13}C NMR (75 MHz, $CDCl_3$, ppm) 142.1, 119.9, 31.8, 29.6, 29.3, 28.8, 22.7, 14.1.

3,4-Dioctylthiophene (19d)

Prepared according to general procedure. Colorless oil was obtained in 70% yield. ^{1}H NMR (300 MHz, $CDCl_3$, ppm) 6.85 (s, 2H), 2.51 (t, J = 6.9 Hz, 4H), 1.61 (m, 4H), 1.26 (m, 20H), 0.88 (s, 6H). ^{13}C NMR (75 MHz, $CDCl_3$, ppm) 142.0, 119.9, 32.0, 29.8, 29.6, 29.5, 29.4, 28.9, 22.8, 14.1.

General Procedure for Synthesis of 2,5-Bis(2'-thienyl)-3,4-dialkylthiophene (21)

The following compounds were synthesized using the following procedure, altered from a literature source.[83] Under argon, DMF is stirred with **20** (1 eq), $PdCl_2(PPh_3)_2$ (0.05% mol eq), LiCl (5 eq), and 2-(tributyltin)-thiophene (2.8 eq). Mixture is refluxed for 48 hours, then cooled to room temperature, extracted with hexanes and washed three times with water. Solvent is then removed to produce a green oil that is purified by silica column chromatography using hexanes as the eluent.

2,5-Bis(2'-thienyl)-3,4-dibutythiophene (21b)

Prepared according to general procedure. Yellow-green oil was obtained in 74% yield. ^{1}H NMR (300 MHz, $CDCl_3$, ppm) 7.27 (d, J = 3.9 Hz, 2H), 7.12-7.05 (m, 4H), 2.70 (t, J = 6.6 Hz, 4H), 1.60-1.34 (m, 8H), 0.94 (s, 6H). ^{13}C NMR (75 MHz, $CDCl_3$, ppm) 140.0, 136.2, 129.8, 127.3, 125.8, 125.2, 32.9, 27.8, 23.0, 13.8.

RESULTS/DISCUSSION

The synthesis of (**18**) was undertaken in an attempt to create oligothiophenes with morphological properties similar to that of liquid crystals. To this end, the synthesis was considered through numerous avenues, the seemingly most effective being represented in Scheme 5. The initial step was based on a literature preparation of the singly substituted thiophene,[84] and the work of Brown, *et al.* with actual liquid crystals[76] inspired the final scheme in order to continue progress even with singly substituted thiophenes. Work was completed successfully through compound **17**, and difficulties were encountered in the characterization of **18** due to insufficient purification by column chromatography.

Prior to the execution of this plan, the hydroxylation of 3,4-dimethylthiophene was considered in order to keep in line with the other proposed molecules of this project. This approach, however, was avoided due to the inaccessibility of the starting material, which was not commercially available and could be synthesized either through three or more steps,[85,86] or through the use of 90% hydrogen peroxide.[87] The former pathway was considered highly inefficient and the latter a last resort due to danger of working with this chemical. Successful disubstitution of liquid crystal moieties will thus have to proceed through a different pathway.

The outlined process in Scheme 6 captures the optimum conditions found for the synthesis of these sexithiophenes through a traditional approach. In fact, many studies based on similar structures corroborate specific details of our work, such as the use of

2,5-dibromothiophene rather than 2,5-diiodothiophene.[52] The synthesis of the terthiophene structure through a Grignard reaction has been recorded, and may be a worthwhile method for carrying out this scheme with fewer side products.[62] Major improvements to the above synthesis would thereby require replacing the entire process with a different scheme, two possibilities of which are outlined in the Future Directions below.

The straight alkyl chain substitution on sexithiophenes (Scheme 6) was initially limited to the creation of **22a** and **22b** in order to compare the synthetic process of a novel compound and that of a known one, respectively. The dibutyl terthiophene structure (**21b**) was successfully synthesized, but the corresponding sexithiophene was difficult to separate from the numerous side products of the reaction, leaving an impure sample. Progress on compound **22a** has been completed through **20a**, and the subsequent reactions will likely follow the route of **22b** synthesis quite closely. Complications of the reaction conditions for **20a-d** are centered on some published preparations calling for a dark setup, and some not. An examination of the difference in yields with either method revealed higher yields when this reaction is run in the dark. Preparations for the shorter chains (**20a-b**) do not mention this step, whereas those of **20c** do.

The process for the neopentyl group substitution through ring closure was successful in producing compound **24**; the following reaction, however, had zero conversion over multiple attempts. This was especially disappointing given the reported 78% yield and X-ray single-crystal structure analyzed for this process.[72] Given this lack of success, the synthesis of 3,4-dicyclohexylthiophene was approached through a Grignard reaction as with compounds **19a-d**, but this also yielded no product. Upon the attachment of neopentyl and cyclohexyl groups to the center thiophene rings of the corresponding sexithiophenes, the resulting compounds would require bromination for

the creation of terthiophene structures. These reactions can be completed following the preparations of other researchers who have succeeded in performing similar activations.[88]

FUTURE DIRECTIONS

The opportunity to successfully imitate the properties of liquid crystals in sexithiophene molecules may be appropriated through the use of a scheme carried out by K Guo *et al*.[89,90] in the synthesis of novel diazo chromophores. Through the creation of diethyl thiodiglycollate, this group successfully synthesized and characterized 3,4-dibutoxythiophene. Because our first target of a liquid crystal moiety on sexithiophene is based on exploration, the absence of a methylene group between the oxygen and thiophene ring in 3,4-dibutoxythiophene should not pose a problem for the aims of this project. Futhermore, the use of a hexyl instead of butyl chain could likely be completed just as successfully.

The improvement of yields and limitation of side products is crucial in isolating the final sexithiophene products of our project. Both of these obstacles have presented themselves in the final coupling step (Scheme 6) of our pathway. One possibility for improvement is the testing of different reaction conditions, or an exploration of different catalysts at the very least. These same conditions, for example, have been utilized for the coupling of terthiophenes through the use of (dppf)$PtCl_2$ and (dppp)$PtCl_2$ with great success.[91]

For the general improvement of our overall sexithiophene progress, it may be worthwhile to follow the solvent-free microwave-assisted synthetic pathway we adopted for the Suzuki-Miyaura coupling resulting in compound **6**. Exact conditions have actually been carried out by Melucci, *et al*., for the synthesis of thiophene oligomers, and was especially helpful in controlling the presence and type of side products, thereby increasing yields through multiple avenues.[52] Unlike our success with benzothiadiazole and fluorene coupling, the optimized conditions for terthiophene synthesis included the use of $PdCl_2$(dppf) as catalyst, resulting in a 73% yield.[52] Not only is this a significantly higher yield than our yield for compound **22b**, but it was accomplished with shorter reaction times and a drastic reduction in amounts of solvent used. This method is even more attractive for future use in our project given that this research group successfully synthesized 4”,3’’’-dimethyl-2,2’:5’,2”:5”,2’’’:5’’’,2’’’’:5’’’’,2’’’’’-sexithiophene in much higher yields than through Stille coupling.[52] Our F8BT project may also provide synthetic inspiration in the form of solid phase synthesis. SPS has been used for the synthesis of benzothiazole and thiophene derivatives, [35] and could reduce the continued difficulty of isolating the final alkylsexithiophenes (**22**). Because of thoroughly different nature of this approach, it should be performed only in the event the above modifications do not provide success in producing the target molecules of this project (

Table 2).

Chapter 3: Synthesis of Conducting Metallopolymers for Electrostimulated Delivery of Nitric Oxide

INTRODUCTION

Recent innovations in controlled drug release have resulted in many new forms of administration, including implants with the ability to release a drug to the body over a given period of time, such as a day or even several years.[92] New systems also include a non-invasive transdermal drug delivery method called iontophoresis, in which an applied electrical current forces the delivery of a medication into the skin.[93] These systems often take advantage of the membrane and reservoir properties of conducting polymers in order to fulfill these tasks.[94] CPs have been selected as drug carriers due to the ease with which they can be synthesized and structurally modified for specific applications.[95] In particular, electroactive CPs, such as those employed in iontophoresis, have shown promise as drug carriers since their redox properties allow for controlled electron transport through the polymer backbone.[96]

Development in the field of drug delivery has led researchers to hone in on the valuable properties of CPs that can be manipulated for this purpose, the most direct of which is molecular swelling. A change in the electronic charge of a conducting polymer leads to a change in the ionic charge, the latter of which requires a mass transport between the polymer and electrolyte.[94] This forces the incorporation of counter ions into the polymer, expanding its size.[94] Conversely, the release of the counter ions will contract the polymer.[94] Compounds such as salicylate, ferrocyanide, and glutamate have been successfully entrapped into polymer membranes and then released upon reduction.[96] This property allows for drug release systems built on CPs to be externally triggered through changes in redox state.

One example of such a system is the precise, controlled release of anti-inflammatory drugs for treating the inflammatory response of neural prosthetic devices, which is required at specific points in time.[94] Research efforts on this and other systems are focused on creating within the material a reservoir from which the bioactive molecules can be supplied to the host system at a controlled rate and period of delivery.[96] A drawback to this basic approach of incorporation and release is the possibility of spontaneous drug release, a reality that has hampered major development with this method. One alternative is the use of bilayer systems in which two physically segregated CP thin films assure more control over the incorporated molecule.[96] Another possibility is the physical entrapment or covalent binding of the key molecules, a technique that has been used in the immobilization of enzymes, antibodies, and even whole living cells.[96]

Drug delivery systems based on polymeric materials are an optimum form of administration because they can delivery to a precise region of the body where it is physiologically needed. This form of administration is efficient in terms of the amount of drug used and provides increased effectiveness. It also lowers the risk of side effects for the patient and reduces recovery time. The development of drug delivery systems with these advantages over conventional medicines is thus an invaluable effort in the pharmaceutical industry.

The project described herein is based on a molecular immobilization technique, but utilizes the reversible binding abilities of metals within CPs in order to provide a direct bond to the desired drug. This allows for the electrochemical triggering while avoiding spontaneous drug release. Moreover, it creates the possibility of employing the system within an implanted electrical device in order to control the amount and rate of delivery. The small molecule release model in Figure 13 illustrates the weakening of the metal-ligand bond upon electrical doping that will eventually cause a release of the

ligand. The ligand of interest in this case is nitric oxide, the main component of drugs used in the treatment of heart attacks and angina.

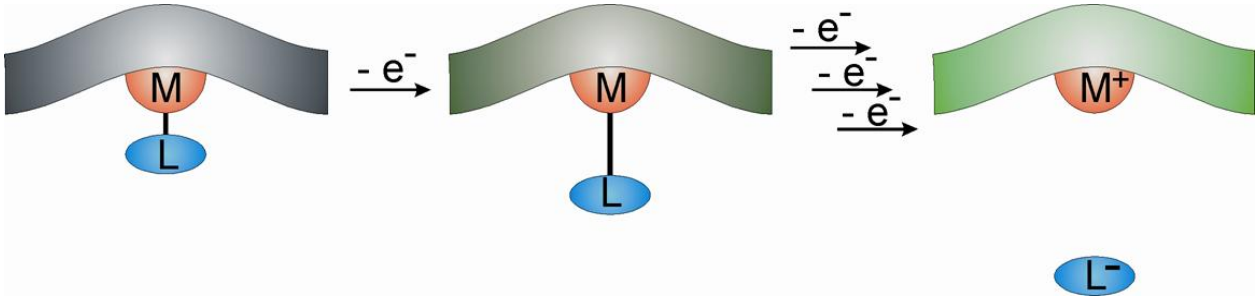

Figure 13. Small molecule release model.[97]

Given the urgent nature of a heart attack, direct treatment would mean less harm endured by the patient. Quickly restoring blood flow to the heart after an attack has been found to minimize damage to the body and increases the chance of patient survival.[98] One current treatment for heart attacks is the administration (by pill, IV, cream, or patch) of nitroglycerin; this supplies nitric oxide to the smooth muscle of the heart, signaling the muscle to relax, which in turn dilates arteries and increases blood flow. As the ligand in a CP drug delivery system like the one outlined above, NO would be directly released to the target area upon an electrical trigger from a device similar to a pacemaker. In p-doping the polymer backbone, electron density is pulled away from the metal center. Due to back-bonding, this action causes the M-NO bond to weaken. Thus, the release of NO in our system is based on a degradation of its bond to the metal and not a direct cleavage. This direct treatment would help avoid permanent damage for the patient while en route to the care of a hospital. This device would conceivably be preemptively implanted in a patient who is at high risk for a heart attack.

The development of a CP with the ability to release NO for the treatment of heart attack and angina has been undertaken. Originally, this system was based on the *N, N*-

(2,2'-dimethoxydiphenyl)amine (**25** in Scheme 8, later revised to Scheme 9), but this was later replaced with 2,6-bis(*N*-pyrazolyl)pyridine (**26,** Scheme 10). Through the bilateral attachment of bithiophene or 3,-4-ethlenedioxythiophene (EDOT), this ligand is able to be polymerized. Complexation with a transition metal will allow this electroactive polymer to attach 1-3 NO molecules per monomer. Because the incorporation of counterions into a CP during the doping process leads to weaker bonds, we have focused on metallation of the ligand structure prior to electrochemical polymerization.

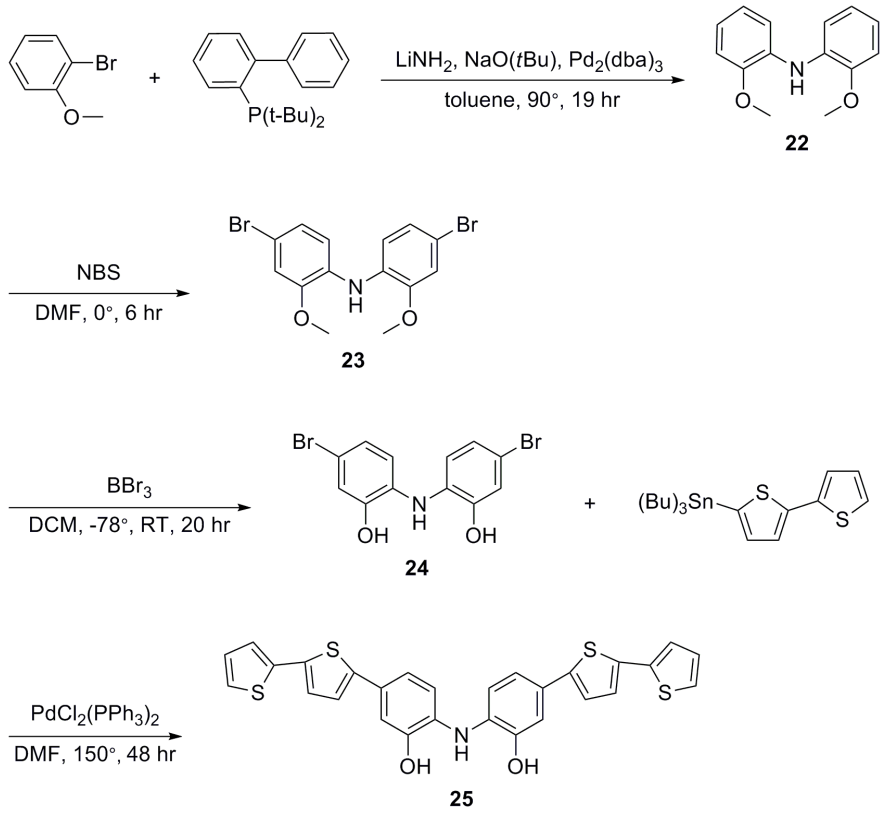

Scheme 8. Originally targeted ligand.

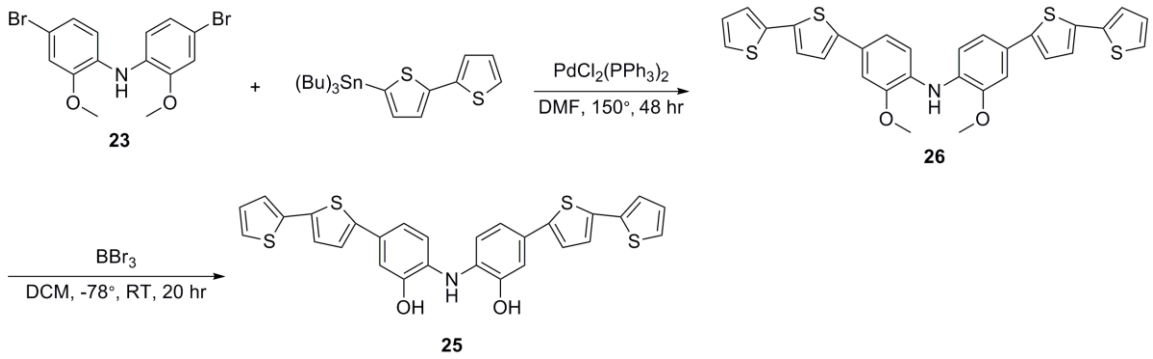

Scheme 9. Revised ligand synthesis.

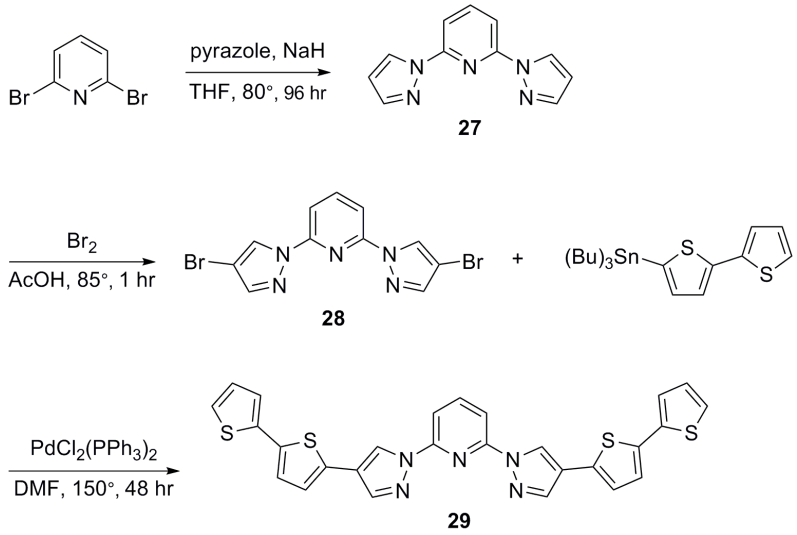

Scheme 10. Newly targeted ligand synthesis.

After the synthesis of the basic ligand, the process continues with the end goal of producing a metallic complex bound firstly to carbon monoxide, then nitric oxide. CO is a preferred stepping-stone to NO due to its lower levels of toxicity and expense. These two compounds are also isoelectronic and, in comparable circumstances, form equally strong bonds with transition metals. Because both NO and CO are π-acceptors, the completed system should function similarly with either ligand. With many of our targeted metals, it is possible to employ a starting material containing CO in order to

avoid unnecessary steps. This would then be switched to NO through literature procedures incorporating the nitrosylating agent *N*-nitroso-*N*-methyl-*p*-toluenesulfonamide ("Diazald")[99] or $NOPF_6$.[100]

The number of NO ligands in the complex, as well as their bonding mode, will vary based on the nature of the coordinated metal and its oxidation state. For a neutral compound to be formed with the original ligand, the attached metal would need to be in a $^{+}3$ oxidation state given that each of the two oxygen atoms and the nitrogen atom are of $^{-}1$ charge and the neutral NO will not impact the oxidation state of the metal. The revised target ligand, however, is neutral, and thus requires the inclusion of an electronegative ligand and/or counterion to counteract a positive metal charge. The choice of metal depends on numerous factors, not the least of which is the requirement that it be a metal with redox potentials compatible with the binding of NO. The bonding and oxidation details of some of the metals originally considered are outlined in Table 3. As can be seen, a large range of possible oxidation states (namely I, II, III, and IV) allows for numerous options of transition metals with which to form the target complex.

Another major factor in considering metals for complexation is the predicted reactivity of the ligand based on the Hard/Soft Acid/Base Theory. For the purpose of synthesizing our target molecules, the classification of C_5H_5N as a borderline hard/soft base allows for the consideration of numerous metals. Iron, nickel, cobalt, chromium, and manganese were immediate targets given their ease of use and relatively low cost. The scope was further broadened by the existence of many metal carbonyl complexes that are commercially available. These include rhenium, tungsten, platinum, and rhodium.

Metal	Coordination Number	Electron Count	Linear NO Molecules	Bent NO Molecules	Favorable Oxidation States
Chromium	7	18	2	2	II
	6	17	2	1	II, III, IV
	5	16	2	0	II, III, IV
Manganese	6	18	2	1	II, III
	5	17	1	2	II, III
Iron	7	18	2	0	II, III
	5	18	1	3	III
Cobalt	6	18	1	2	I, II, III, IV
	5	17	1	1	I, II, III
	4	16	1	0	I-, 0, I, II, III, IV, V
Nickel	6	17	0	3	II, III, IV
	5	16	0	2	II, III
		18	1	1	II, III
	4	17	1	0	0, I, II

Table 3. Possible bonding modes for select transition metals.

The variations in common bonding geometries of these metals offer many possible conformations for our final complex. The predicted number of NO molecules for binding each metal in Table 3 is based on a stable electron count for the common geometries of each metal, as well as the known existence of metal compounds containing NO molecules bound in both a bent and linear fashion. When predicting the binding modes of NO, it is important to bear in mind the common coordination patterns for each

metal as well as its common oxidation states. For example, the most stable and important oxidation states of chromium are II and III, while the latter in an octahedral conformation is the most stable chromium structure. Hexa- and penta-coordinate manganese complexes will also be possible given the stability of Mn^{II}. The first step in the determination of structure, however, is the selection of carbonyl starting material, which will dictate the possible resulting NO complexes of our structures.

EXPERIMENTAL

All chemicals used in the following reactions were obtained through commercial sources and used received. Solvents were dried using a Pure-Solv 400 solvent purification system. ^{1}H and ^{13}C NMR were obtained on a Varian Unity+ 300 and were referenced to the residual solvent peaks. HRMS was carried out on a Thermo Finngan TSQ 700. Literature methods were followed for the preparation of bis-(2-methoxy-phenyl)-amine (**22**),[101] 2,6-bis(*N*-pyrazolyl)pyridine (**27**),[102] and 2,6-bis(4-bromopyrazol-1-yl)pyridine (**28**).[103]

All spectroscopic data was obtained in DCM solutions unless otherwise noted. Absorption spectra were recorded on a Varian Cary 6000i UV-VIS-NIR Spectrophotometer with Starna Quartz Fluorometer Cells with a pathlength of 10 mm. Luminescent measurements were recorded on a Photon Technology International QM 4 spectrophotometer equipped with a 6-inch diameter K Sphere-B integrating sphere. Electrochemical syntheses and studies were performed in a dry-box under a nitrogen atmosphere using a GPES system from Eco. Chemie B.V. All the electrochemical experiments were carried out in a three-electrode cell with $Ag/AgNO_3$ reference electrode (silver wire dipped in a 0.01 M silver nitrate solution with 0.1 M Bu_4NPF_6 in CH_3CN), a Pt working electrode, and Pt wire coil counter electrode. Potentials were relative to this 0.01 M $Ag/AgNO_3$ reference electrode. Ferrocene was used as an external reference to

calibrate the reference electrode before and after experiments were performed and that value was used to correct the measured potentials. All electrochemistry was performed in dichloromethane (DCM) solutions using 0.1 M [(*n*-Bu)$_4$N][PF$_6$] (TBAPF$_6$) as the supporting electrolyte. The TBAPF$_6$ was purified by recrystallization three times from hot ethanol before being dried for 3 days at 100-150 °C under active vacuum prior to use. Polymer films were prepared on Delta Technologies ITO-coated glass for spectroscopic measurement and on stainless steel for XPS. Electrosyntheses of the polymer films were preformed from 1 x 10^{-3} M monomer solutions by continuous cycling between -1.5 V and 1.5 V at v = 100 mVs^{-1}. The films obtained were then washed with fresh DCM before further experiments.

Bis-(4-bromo-2-methoxy-phenyl)-amine (23)

Synthesized by adapting a procedure from literature[104] starting with compound **10**. ^{1}H NMR (300 MHz, $CDCl_3$, ppm) 7.14 (d, J = 8.7 Hz, 2H), 6.99 (d, J = 6.6 Hz, 4H), 6.36 (s, 1H), 3.84 (s, 6H). ^{13}C NMR (75 MHz, $CDCl_3$, ppm) 150.0, 131.5, 123.8, 116.7, 114.4, 112.4, 56.3. HRMS (CI+) *m/z* calculated for $C_{14}H_{13}NO_2Br_2$ $(M + H)^+$ 384.9319, observed 384.9313.

Bis-(4-bromo-2-hydroxy-phenyl)-amine (24)

Synthesized according to literature procedure[105] starting with compound **10**. ^{1}H NMR (300 MHz, $CDCl_3$, ppm) 7.05 (s, 2H), 6.96 (d, J= 6.9 Hz, 2H), 6.69 (d, J=8.4, 2H), 5.71 (s, 1H), 5.42 (s, 1H). ^{13}C NMR (75 MHz, $CDCl_3$ ppm) 148.7, 130.3, 124.4, 121.6, 118.4, 115.6. HRMS (CI+) *m/z* calculated for $C_{12}H_{10}NO_2Br_2$ $(M + H)^+$ 357.9080, observed 357.90728. Anal. Calcd: C, 40.15; H, 2.53; N, 3.90. Found: C, 40.02; H, 2.44; N, 3.78.

Bis(4-(2,2'-bithiophen-5-yl-2-methoxyphenyl)amine (26)

Synthesized using a procedure in literature[83] starting with 1 equivalent each of **24** and 5-(Tributylstannyl)-2,2-bithiophene). . ^{1}H NMR (300 MHz, $CDCl_3$, ppm) 7.42 (s, 2H), 7.29-7.10 (m, 12H), 7.05 (dd, *J*=3.2, *J*=1.5, 2H), 4.01 (s, 6H). HRMS (CI+) *m/z* calculated for $C_{30}H_{23}NO_2S_4$ $(M + H)^+$ 557.06, observed 558.09.

2,6-Bis(4-(2,2'-bithiophen-5-yl)-1*H*-pyrazol-1-yl)pyridine (29)

Synthesized according to literature[83] starting with compound **6**. ^{1}H NMR (300 MHz, $CDCl_3$, ppm) 8.72 (d, *J*=0.6 Hz, 2H), 7.95-7.93 (m, 2H), 7.89-7.86 (m, 3H), 7.23-7.19 (m, 4H), 7.15-7.13 (m, 4H), 7.03 (dd, *J*=3.6, *J*=1.2, l2H).

RESULTS/DISCUSSION

The synthetic route for the originally targeted ligand of the NO drug-release system is displayed in Scheme 8. Prior to the illustrated reaction conditions, the synthesis of compound **22** was initiated by a preparation based on the Jordan-Ullmann synthesis.[106] The starting materials in this paper varied in the substituents on the phenyl ring; their difference in reactivity from the bromoanisole shown is the likely the reason for the ineffectiveness of this approach. Once adopting the palladium-catalyzed route, the process was halted once more at the attempt to remove the terminal methyl group of compound **23**. The synthesis was thus revised to postpone this removal until after the addition of the bithiophene (Scheme 9). While the new approach was successful in creating the polymerizable compound **26**, the consequential attempts to cleave the methyl group were ineffective. Because these hydroxyl groups would serve as two of the arms of the chelating ligand (with the phenyl-bridging nitrogen as the third), this step is crucial in the incorporation of a metal into the system.

This setback, as well as published studies of its metal complexes, revealed the unsuitability of this ligand for the purpose of this project. The hydroxyl structure of the ligand proposed in Scheme 8 and Scheme 9 is known to function as an *o*-quinone ligand, an electroactive ligand that can be found as neutral quinones, radical semiquinones, or dianionic catecholates (Figure 14).[107] When bound to a metal, compound **25** thus forms a Schiff base with three valence tautomeric isomers.[108] The numerous oxidation states of these metal complexes allow them to exhibit rich electrochemical activity. It is likely then, that in the attempts to cleave the terminal methyl group, the reactivity of the hydroxyl groups decreased the stability of the product. This ligand was further disqualified as a basis for this project given the ease with which external stimuli (such as temperature and pressure) can cause interconversion between the oxidation states.[108]

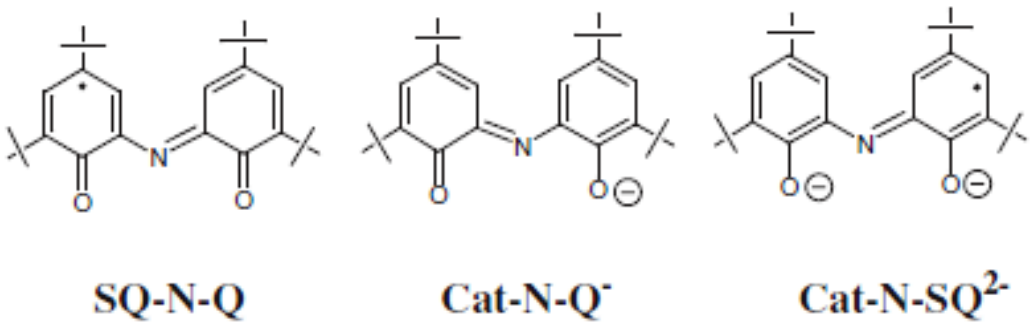

Figure 14. Example of similar Schiff base ligand and its three possible oxidation states. Q= neutral quinone, SQ^{-}= radical semiquinone, Cat^{2-}= dianionic catecholate.

The target ligand was thus changed to compound **29** in order to avoid additional electrical activity that might interfere with the desired small-molecule release mechanism. After successful synthesis of the ligand, complexation was attempted with a variety of metal salts (Table 4). While solvents and additional reagents varied from reaction to reaction, all attempts listed were run in argon-sparged solvent and refluxed for a period of 1-96 hours, depending on the nature of the metal. Entries 1- 5 and 11-12

outline metalliation reactions that had zero conversion and all starting material was able to be retrieved from solution.

Entry	**Metal Salt**	**Solvent**
1[110]	$Cr(CO)_6$	Benzene
2[111]	CuI	THF[a]
3[112]	$FeCl_2 \bullet 4H_2O$	*n*-butanol
4[113]	K_2PtCl_4	H_2O
5[114]	$Pt(COD)Cl_2$	H_2O: MeOH
6[115]	$ReBr(CO)_5$	toluene[b, c]
7[116]	$ReBr(CO)_5$	H_2O[c]
8[117]	$[Re(CO)_3(H2O)_3]Br$	H_2O
9[118,119]	$[NEt_4]_2[ReBr_3(CO)_3]$	2-methoxy-ethyl-ether
10[120]	*fac*-$[Re(CO)_3(dmso\text{-}O)_3(F_3SO_3)]$	acetone: DMSO
11[121]	$RuCl_3 \bullet 3H_2O$	Ethoxyethanol
12[109]	$W(CO)_6$	*n*-octane

Table 4. Metallation reaction conditions for compound **29**; a) reacted with CO(g); b) also conducted in dry DCM; c) reacted with $AgPF_6$ or $NaPF_6$.

The published preparation of the tungsten carbonyl complex includes details about the large activation barrier of this reaction.[109] An extended reflux period was recommended for compounds that are more difficult to metallate, so our preparation with ligand **29** began with 48 hours of reflux, and was later extended to 96 hours. Progress was followed by TLC, which displayed only starting materials every time. With the platinum metallation, however, progress was tracked qualitatively through the anticipated precipitation of the red complex. Unfortunately, the dark orange precipitate did not display a shifted NMR spectrum from that of the ligand alone. The iron complexation

also showed no visible or spectral changes, but showed some promise when reacted slowly by layering the two materials in a large test tube. While the resulting crystals did not diffract, this proved to be a method worth exploring with other metal salts.

The first rhenium reaction attempted made use of $ReBr(CO)_5$ with the goal of extracting the bromine from the starting material prior to reaction with the ligand, or after complexation. Through static and dynamic ^1H NMR studies, Garcia, *et al.* discovered the products of less complex 2,6-bis(*N*-pyrazolyl)pyridine (bbpy) ligands with $[ReBr(CO)_5]$ were fluxional.[115] By comparing metallated bbpy ligands with various asymmetric and symmetric geometries, they were able to elucidate the "tick-tock" conformational changes present in these complexes. It was assumed then, that our symmetric modification of the bbpy ligand would also produce fluxional molecules that, at room temperature, would alternate back and forth in Re-N attachments and appear as a single molecule by ^1H and ^{13}C NMR. The objective of removing the bromine from the starting material or resulting complex was to avoid this flux in conformation and force a tridentate binding of the rhenium atom.

Initially, the reaction was conducted in argon-sparged toluene, then in argon-sparged water, both of which resulted in zero conversion. Given the possibility of an air-sensitive intermediate, the reaction was then carried out in a glovebox with dry DCM. For the purpose of removing the bromine ligand, $ReBr(CO)_5$ was first stirred with $NaPF_6$ at room temperature for an hour. This mixture was filtered and added to ligand **29** dissolved in DCM. Every repeated attempt produced an almost instantaneous thickening of the solution, followed by the precipitation of yellow solid. Given the appearance of this product, reaction samples were then stirred for different lengths of time, ranging from 2-48 hours, but not refluxed.

While there were variations in color solution between yellow and green, the crude products of these reactions were essentially the same. Purification was first attempted by column chromatography with silica gel to separate two fractions found by TLC, one of which was the starting ligand. However, decomposition by this method was assumed based on a vast change in color intensity and the return of only starting material. Recrystallization in a variety of solvents was then attempted for the isolation of the second, more luminescent fraction. The optimum combination of solvents was found to be hexanes and DCM, which precipitated a mustard-color solid that was bright yellow-orange in solution.

Purification proved difficult, however, as both the precipitated solid and the filtrate appeared as starting material by TLC, and the formerly present fraction was no longer in the mixture. Chromatography was abandoned as a method of purification due to the possibility of complex decomposition. The yellow solid was characterized by electrochemistry (Figure 16) and fluorescence spectroscopy (Figure 17B), both of which produced almost identical data to that of the ligand alone (Figure 15, Figure 17A). Most importantly, a fluorescence peak between 500 and 600 nm indicating the presence of the rhenium atom is absent from these plots. Thus, it was concluded that either the complex decomposed soon after completion of the reaction, or it was never produced. Table 4 lists other rhenium starting materials used for the complexation of **29**: $[Re(CO)_3(H_2O)_3]Br$, $[NEt_4]_2[ReBr_3(CO)_3]$, and *fac*-$[Re(CO)_3(O\text{-dmso})_3(CF_3SO_3)]$. These required further processing of $ReBr(CO)_5$ in order to obtain starting materials more likely to bind our ligand.[117,118,119] However, these reactions also resulted in zero conversion.

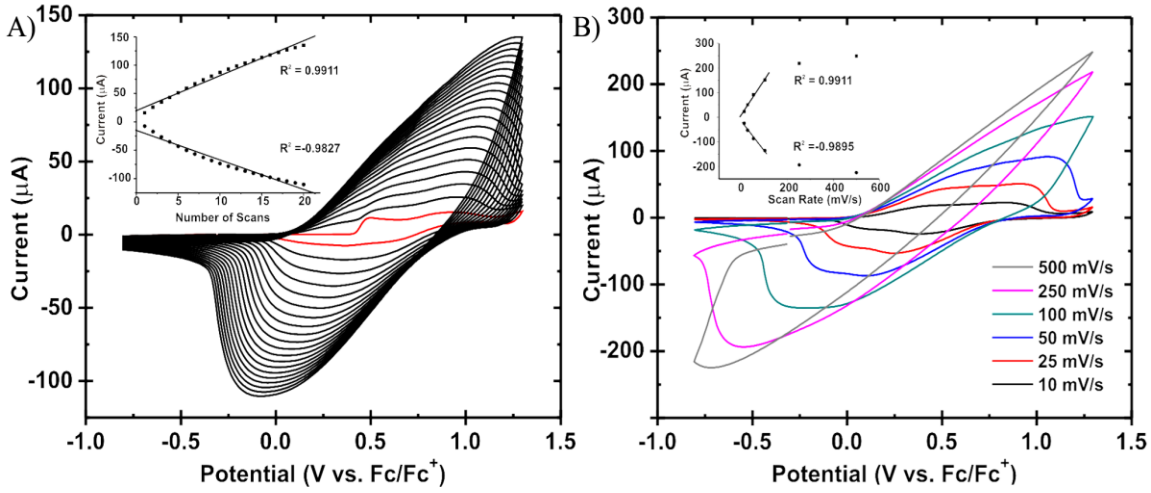

Figure 15. a) Cyclic voltammogram of **28**. Inset: plot of current versus number of scans. b) Scan rate dependence study of **28**. Inset: plot of current versus scan rate.

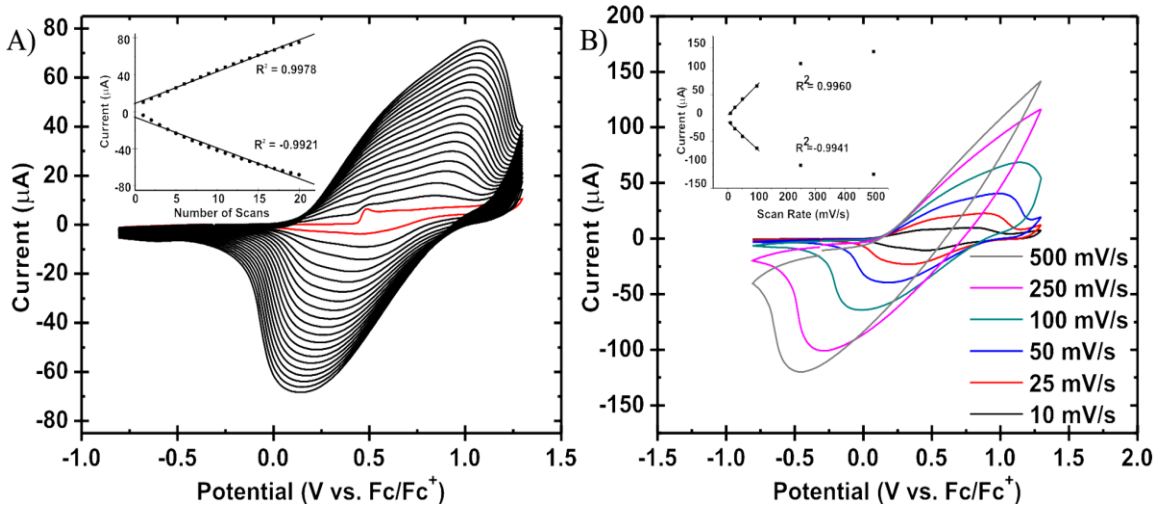

Figure 16. a) Cyclic voltammogram of the reaction product when attempting to make **29**. Inset: plot of current versus number of scans. b) Scan rate dependence study of the reaction product when attempting to make **29**. Inset: plot of current versus scan rate.

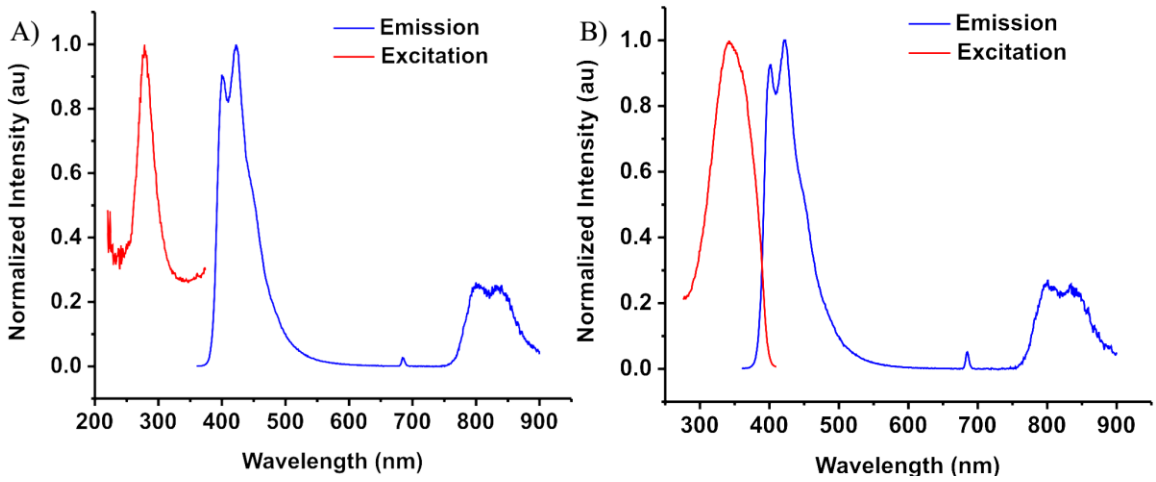

Figure 17. a) Photophysics of **28**. b) Photophysics of the reaction product when attempting to make **29**.

FUTURE DIRECTIONS

These various metallation attempts provide some promising approaches toward the synthesis of the desired metal compounds. Future reactions with $Re(CO)_5$ should continue to be run in the glovebox, but should also be followed by refluxing of at least two hours. Column chromatography should continue to be avoided, as well as TLC plates as an adequate method of tracking reaction progress. Future purification of crude materials should only be based on recrystallization, and care should be taken to keep all final products in the absence of light, in case this proves to be an avenue of decomposition.

One possible roadblock in the future of this project is difficulty in displacing the carbonyl ligands from the final metal complexes. It is likely that the effectiveness of nitrosylation will vary greatly by the type of metal present in the final product. The sequence of isoelectronic and isostructural first row transition metal molecules

$Co(NO)(CO)_3$, $Fe(NO)_2(CO)_2$, $Mn(NO)_3CO$, and $Cr(NO)_4$ indicate this variance of carbonyl replacement.[99] It may be worthwhile then, to focus metallation efforts on manganese and chromium when using first row transition metals. Xu, *et al.* also found the metal-carbonyl bond with rhenium to be stronger than the corresponding bond with first and second row metals Unfortunately, this resulted in the liberation of carbonyl and subsequent nitrolysation of $Re(CO)_5$ only progressing to $Re(NO)(CO)_4$.[99] If sequential nitrolysation reactions are not successful with the above rhenium complex, it may be necessary to leave out this metal as a possible target. If nitrolysation efforts are unfruitful overall, an alternative pathway would include originally metallating with nitrosyl metal salts.

Conclusion

The high potential for metal complexation with the proposed bbpy ligand points to numerous options of metallopolymers for the project described in Chapter Three. Maximization of NO release through this synthesis and optimization of the system in the hands of collaborating engineers will ensure the finalization of one of these compounds for the purpose of drug delivery. The successful creation of these NO-releasing metallopolymers is a promising start to the creation of a life-saving device for victims of heart attacks and a relief for suffers of chronic angina. Furthermore, this novel approach toward small molecule release would likely be great precedent for future exploration into other electronic and medical applications.

The studies exploring the effects of various attachments on the morphology of oligothiophenes are also a promising avenue in the field of semiconducting materials. The improvement of conductivity through alteration of crystal packing and material-substrate interaction will open many possibilities for device fabrication. The compounds described in Chapter Two will likely be the jumping off point in the creation of a library of unique and tailored oligothiophenes. They are great start in a large area of possible development given the prominence of thiophenes in the front lines of devices such as photovoltaics and light-emitting diodes.

The F8BT oligomer project described in Chapter One will open doors in defining the relationship between structure and electrical activity. The involvement of modern techniques such as single-molecule spectroelectrochemistry will especially be helpful in learning more about these compounds and other fluorene polymers that are widely used in the field of electronic devices. Furthermore, establishing the details of size for

optimum conductivity could potentially lead to efficient use of materials and greater accessibility of effective material design.

The exploration into these three projects described above took advantage of the many beneficial properties of structure optimization, metallation, and polymerization. Through the use of major characterization techniques, such as crucial electrochemical measurements, the study of these conducting polymer systems was tracked for efficiency and progress. The implications of these approaches to the improvement of electrical devices are numerous; the continuation of these methods will likely produce major changes in the field of CP morphology and resulting device function. The utility of organic semiconducting materials within these anticipated applications will form a substantial component of future research and development.

References

(1) Horowitz, G. In *Semiconductin Polymers: Chemistry, Physics and Engineering*; Hadziioannou, G., Van Hutten, P. F., Eds.; Wiley-VCH: Weinheim, 2000, p 463-514.

(2) Bernius, M. T.; Inbasekaran, M.; O'Brien, J.; Wu, W. *Adv. Mater.* **2000**, *12*, 1737-1750.

(3) McCullough, R. D.; Lowe, R. D.; Jayaraman, M.; Anderson, D. L. *J. Org. Chem.* **1993**, *58*, 904-912.

(4) Haddon, R. C.; Kaplan, M. L.; Wudl, F.; Sibley, S. P. In *Kirk-Othmer Encyclopedia of Chemical Technology*; 3rd ed.; John Wiley & Sons, Inc.: 2000; Vol. 20, p 674-698.

(5) Dibbs, M. G.; Brennan, D. J.; Garrou, P. E.; Shaw, J. M. *Proc. SPIE-Int. Soc. Opt. Eng.* **2004**, *5520*, 90-97.

(6) Burroughes, J. H.; Bradley, D. D. C.; Brown, A. R.; Marks, R. N.; Mackey, K.; Friend, R. H.; Burns, P. L.; Holmes, A. B.; *Nature* **1990**, *347*, 539-541.

(7) Graupner, W.; Tasch, S.; Leising, G. In *Semiconducting Polymers: Chemistry, Physics and Engineering*; Hadziioannou, G., van Hutten, P. F., Eds.; Wiley-VCH: Weinheim, 2000, p 259-307.

(8) Kline, R. J.; DeLongchamp, D. M.; Fischer, D. A.; Lin, E. K.; Heeney, M.; McCulloch, I.; Toney, M. F. *Appl. Phys. Lett.* **2007**, *90*, 062117/1-062117/3.

(9) Johansson, E.; Larsson, S. *Synth. Met.* **2004**, *144*, 183-191.

(10) Liem, H.; Etchegoin, P.; Whitehead, K. S.; Bradley, D. D. C. *J. App. Phys.* **2002**, *92*, 1154-1161.

(11) McCulloch, I.; Heeney, M.; Bailey, C.; Genevicius, K.; MacDonald, I.; Shkunov, M.; Sparrow, D.; Tierney, S.; Wagner, R.; Zhang, W.; Chabinyc, M. L.; Kline, R. J.; McGehee, M. D.; Toney, M. F. *Nat. Mater.* **2006**, *5*, 328-333.

(12) Brabec, C. J.; Sariciftci, N. S. In *Semiconducting Polymers: Chemistry, Physics and Engineering*; Hadziioannou, G., van Hutten, P. F., Eds.; Wiley-VCH: Weinheim, 2000, p 515-560.

(13) Scott, J. C.; Malliaras, G. G. In *Semiconducting Polymers: Chemistry, Physics and Engineering*; Hadziioannou, G., Van Hutten, P. F., Eds.; Wiley-VCH: Weinheim, 2000, p 411-462.

(14) Sandee, A. J.; Williams, C. K.; Evans, N. R.; Davies, J. E.; Boothby, C. E.; Köhler, A.; Friend, R. H.; Holmes, A. B. *J. Am. Chem. Soc.* **2004**, *126*, 7041-7048.

(15) Bittner, E. R.; Ramon, J. G. S. In *Los Alamos National Laboratory, Preprint Archive, Condensed Matter* 2005, p 1-12.

(16) Liao, J.; Benz, M.; LeGoff, E.; Kanatzidis, M. *Adv. Mater.* **1994**, *6*, 135-138.

(17) Löglund, M.; Salaneck, W. R. In *Semiconducting Polymers: Chemistry, Physics and Engineering*; Hadziioannou, G., Van Hutten, P. F., Eds.; Wiley-VCH: Weinheim, 2000, p 115-148.

(18) Belletête, M.; Mazerolle, L.; Desrosiers, N.; Leclerc, M.; Durocher, G. *Macromolecules* **1995**, 8587-8597.

(19) Profeta, S. In *Kirk-Othmer Encyclopedia of Chemical Technology (online)*; 4th ed.; John Wiley & Sons, Inc.: 2005; Vol. 16, p 315-352.
(20) Dini, D.; Janakiraman, U.; Doblhofer, K. In *Conducting Polymers and Polymer Electrolytes: From Biology to Photovoltaics*; Rubison, J. F., Mark Jr, H. B., Eds.; ACS Washington, 2002, p 103-112.
(21) Murray, M. M.; Holmes, A. B. In *Semiconducting Polymers: Chemistry, Physics and Engineering*; Hadziioannou, G., Van Hutten, P. F., Eds.; Wiley-VCH: Weinheim, 2000, p 1-35.
(22) Charas, A.; Morgado, J.; Martinho, J. M. G.; Alcacer, L.; Lim, S. F.; Friend, R. H.; Cacialli, F. *Polymer* **2003**, *44*, 1843-1850.
(23) Gómez-Romero, P.; Lira-Cantú, M. In *Kirk-Othmer Encyclopedia of Chemical Technology (online)*; John Wiley & Sons, Inc.: 2002; Vol. 13, p 533-561.
(24) Bernius, M.; Inbasekaran, E.; Woo, W. W.; Wujkowski, L. *J. Mater. Sci.* **2000**, *11*, 111-116.
(25) Asawapirom, U.; Guntner, R.; Forster, M.; Farrell, T.; Scherf, U. *Synthesis* **2002**, *9*, 1136-1142.
(26) Belletête, M.; Beaupré, S.; Bouchard, J.; Blondin, P.; Leclerc, M.; Durocher, G. *J. Phys. Chem. B* **2000**, *104*, 9118-9125.
(27) Yim, K.; Friend, R. H.; Kim, J. *J. Chem. Phys.* **2006**, *124*, 184706/1-184706/8.
(28) Bouffard, J.; Swager, T. M. *Macromolecules* **2008**, *41*, 5559-5562.
(29) Herguth, P.; Jiang, X.; Liu, M. S.; Jen, A. K. *Macromolecules* **2002**, *35*, 6094-6100.
(30) Grey, J. K.; Kim, D. Y.; Donley, C. L.; Miller, W. L.; Kim, J. S.; Silva, C.; Friend, R. H.; Barbara, P. F. *J. Phys. Chem. B* **2006**, *110*, 18898-18903.
(31) Xia, R.; Heliotis, G.; Stavrinou, P. N.; Bradley, D. D. C. *Appl. Phys. Lett.* **2005**, *87*, 031104/1-031104/3.
(32) Zheng, Z.; Yim, K.; Saifullah, M. S. M.; Welland, M. E.; Friend, R. H.; Kim, J.; Huck, W. T. S. *Nano Lett.* **2007**, *7*, 987-992.
(33) Xia, R.; Friend, R. H. *Macromolecules* **2005**, *38*, 6466-6471.
(34) Merrifield, R. B. *J. Am. Chem. Soc.* **1963**, *85*, 2149-2154.
(35) Huang, X.; Tang, J. *Tetrahedron* **2003**, *59*, 4851-4856.
(36) Fournier, D.; Pascual, S.; Montembault, V.; Haddleton, D. M.; Fontaine, L. J. *Comb. Chem.* **2006**, *8*, 522-530.
(37) Huang, S.; Tour, J. M. J. *Org. Chem.* **1999**, *64*, 8898-8906.
(38) Kirschbaum, T.; Briehn, C. A.; Bauerle, P. *J. Chem. Soc., Perkin Trans. 1* **2000**, 1211-1216.
(39) Pontrello, J. K.; Allen, M. J.; Underbakke, E. S.; Kiessling, L. L. *J. Am. Chem. Soc.* **2005**, *127*, 14536-14537.
(40) McQuade, D. T.; Pullen, A. E.; Swager, T. M. *Chem. Rev.* **2000**, *100*, 2537-2574.
(41) Palacios, R. E.; Fan, F. F.; Bard, A.; Barbara, P. F. *J. Am. Chem. Soc.* **2006**, *128*, 9028-9029.
(42) Ranger, M.; Rondeau, D.; Leclerc, M. *Macromolecules* **1997**, *30*, 7686-7691.

(43) Grisorio, R.; Mastrorilli, P.; Nobile, C. F.; Romanazzi, G.; Suranna, G. P.; Acierno, D.; Amendola, E. *Macromol. Chem. Phys.* **2005**, *206*, 448-455.
(44) Li, Z. H.; Wong, M. S.; Fukutani, H.; Tao, Y. *Org. Lett.* **2006**, *8*, 4271-4274.
(45) Wang, R.; Wang, W.; Yang, G.; Liu, T.; Yu, J.; Jiang, Y. *J. Polym. Sci., Part A: Polym. Chem.* **2008**, *46*, 790-802.
(46) DaSilveira Neto, B. A. D.; Lopes, A. S.; Ebeling, G.; Goncalves, R. S.; Costa, V. E. U.; Quina, F. H.; Dupont, J. *Tetrahedron* **2005**, *61*, 10975-10982.
(47) Edelmann, M. J.; Raimundo, J.; Utesch, N. F.; Diederich, F.; Boudon, C.; Gisselbrecht, J.; Gross, M. *Helv. Chim. Acta* **2002**, *85*, 2195-2213.
(48) Belfield, K. D.; Schafer, K. J.; Mourad, W.; Reinhardt, B. A. *J. Org. Chem.* **2000**, *65*, 4475-4481.
(49) Jacob, J.; Sax, S.; Piok, T.; List, E. J. W.; Grimsdale, A. C.; Müllen, K. *J. Am. Chem. Soc.* **2004**, *126*, 6987-6995.
(50) Miyaura, N.; Yanagi, T.; Suzuki, A. *Synth. Commun.* **1981**, *11*, 513-519.
(51) Kirschbaum, T.; Azumi, R.; Mena-Osteritz, E.; Bäuerle, P. *New. J. Chem.* **1999**, 241-250.
(52) Melucci, M.; Barbarella, G.; Sotgiu, G. *J. Org. Chem.* **2002**, *67*, 8877-8884.
(53) Korolev, D. N.; Bumagin, N. A. *Tetrahedron Lett.* **2005**, *46*, 5751-5754.
(54) Ding, J.; Day, M.; Robertson, G.; Roovers, J. *Macromolecules* **2002**, *35*, 3474-3483.
(55) Kirschbaum, T.; Bäuerle, P. *Synth. Met.* **2001**, *119*, 127-128.
(56) Faïd, K.; Leclerc, M. *J. Chem. Soc., Chem. Commun.* **1993**, 962-963.
(57) Winokr, M. J.; Wamsley, P.; Moulton, J.; Smith, P.; Heeger, A. J. *Macromolecules* **1991**, *24*, 3812-3815.
(58) Hsu, W.; Levon, K.; Ho, K.; Myerson, A. s.; Kwei, T. K. *Macromolecules* **1993**, *26*, 1318-1323.
(59) Pan, J.; Chua, S.; Huang, W. *Chem. Phys. Lett.* **2002**, *363*, 18-24.
(60) Bao, Z.; Dodabalapur, A.; Lovinger, A. J. *Appl. Phys. Lett.* **1996**, *69*, 4108-4110.
(61) Ukai, S.; Ito, H.; Marumoto, K.; Kuroda, S. *J. Phys. Soc. Jpn.* **2005**, *74*, 3314-3319.
(62) Krömer, J.; Bäuerle, P. *Tetrahedron* **2001**, *57*, 3785-3794.
(63) Fichou, D. *J. Mater. Chem.* **2000**, *10*, 571-588.
(64) Huang, W.; Masuda, G.; Maeda, S.; Tanaka, H.; Ogawa, T. *Chem. Eur. J.* **2006**, *12*, 607-619.
(65) Lovinger, A. J.; Davis, D. D.; Dodabalapur, A.; Katz, H. E. *Chem. Mater.* **1996**, *8*, 2836-2838.
(66) Bäuerle, P.; Würthner, F.; Götz, G.; Effenberger, F. *Synthesis* **1993**, *11*, 1099-1103.
(67) Collings, P. J. *Liquid Crystals: Nature's Delicate Phase of Matter*; Princeton University Press: Princeton, 1990.
(68) Thiemann, T.; Vill, V. In *Handbook of Liquid Crystals*; WIley-VCH: Weinheim, 1998, p 115-132.

(69) Pappenfus, T. M.; Mann, K. R. *Inorg. Chem.* **2001**, *40*, 6301-6307.
(70) Starnes, J., W. H.; Zaikov, V. G.; Chung, H. T.; Wojciechowski, B. J.; Tran, H. V.; Saylor, K. *Macromolecules* **1998**, *31*, 1508-1517.
(71) Nakayama, J.; Yamaoka, S.; Hoshino, M. *Tetrahedron Lett.* **1988**, *29*, 1161-1164.
(72) Nakayama, J.; Hasemi, R.; Yoshimura, K.; Sugihara, Y.; Yamaoka, S. *J. Org. Chem.* **1998**, *1998*, 4912-4924.
(73) Nakayama, J.; Yoshimura, K. *Tetrahedron Lett.* **1994**, *35*, 2709-2712.
(74) Nakayama, J.; Hasemi, R. *JACS* **1990**, *112*, 5654-5654.
(75) Nakayama, J.; Machida, H.; Hoshino, M. *Tetrahedron Lett.* **1985**, *26*, 1981-1982.
(76) Brown, J. W.; Foot, P. J. S.; Gabaston, L. I.; Ibison, P.; Prevost, A. *Macromol. Chem. Phys.* **2004**, *205*, 1823-1828.
(77) Rigenbach, C.; De Nicola, A.; Ziessel, R. *J. Org. Chem.* **2003**, *68*, 4708-4719.
(78) Wurther, F.; Yao, S.; Debaerdemaeker, T.; Wortmann, R. *J. Am. Chem. Soc.* **2002**, *124*, 9431-9447.
(79) Araki, K.; Endo, H.; Masuda, G.; Ogawa, T. *Chem. Eur. J.* **2004**, *10*, 3331-3340.
(80) Diaz-Quijada, G. A.; Weingberg, N.; Holdcroft, S.; Pinto, S.; Pinto, B. M. *J Phys Chem A* **2002**, *106*, 1266-1276.
(81) Bäauerle, P.; Würthner, F.; Götz, G.; Effenberger, F. *Synthesis* **1993**, *11*, 1099-1103.
(82) Haranath, P.; Kumar, V. S.; Reddy, C. S.; Raju, C. N.; Reddy, C. D. *Synth. Commun.* **2007**, *37*, 1697-1708.
(83) Zhu, S. S.; Swager, T. M. *J. Am. Chem. Soc.* **1997**, *119*, 12568-12577.
(84) Taddei, M.; Ricci, A. *Synthesis* **1986**, *8*, 633-635.
(85) Takaya, T.; Hijikata, S.; Imoto, E. *Bull. Chem. Soc. Jpn.* **1968**, *41*, 2532-2534.
(86) Imamoto, T.; Mita, T.; Yokoyama, M. *J. Org. Chem.* **1987**, *52*, 5695-5699.
(87) Ross, D. S.; Moran, K. D.; Malhotra, R. *J. Org. Chem.* **1983**, *48*, 2120-2122.
(88) Thorpe, J. W.; Warkentin, J. *Can. J. Chem.* **1973**, *51*, 927-935.
(89) Guo, K.; Hao, J.; Zhang, T.; Zu, F.; Zhai, J.; Qiu, L.; Zhen, Z.; Liu, X.; Shen, Y. *Dyes and Pigments* **2008**, *77*, 657-664.
(90) Akoudad, S.; Frere, P.; Mercier, N.; Roncali, J. *J. Org. Chem.* **1999**, *64*, 4267-4272.
(91) Zhang, F.; Bäuerle, P. *J. Am. Chem. Soc.* **2007**, *129*, 3090-3091.
(92) Low, L.; Seetharaman, S.; He, K.; Madou, M. J. *Sens. Actuators, B* **2000**, *67*, 149-160.
(93) Fan, Q.; Sirkar, K. K.; Michniak, B. *J. Membr. Sci.* **2008**, *321*, 240-249.
(94) Abidian, M. R.; Kim, D.; Martin, D. C. *Adv. Mater.* **2006**, *18*, 405-409.
(95) Pernaut, J.; Reynolds, J. R. *J. Phys. Chem. B* **2000**, *104*, 4080-4090.
(96) Entezami, A. A.; Massoumi, B. *Iran. Polym. J.* **2006**, *15*, 13-30.

(97) Milum, K. M.; Keskin, S.; Villa, M.; Mejia, M. L.; Holliday, B. J. In *Polymer Preprints (American Chemical Society, Division of Polymer Chemistry)* 2009; Vol. 50, p 333-334.

(98) Stanley J. Swierzewski, I., M.D. In *Cardiology Channel*.

(99) Xu, B.; Li, Q.; Xie, Y.; King, B.; Schaefer III, H. F. *Inorg. Chem.* **2008**, *47*, 9836-9847.

(100) Chung, Y. K.; Sweigart, D. A.; Connelly, N. G.; Sheridan, J. B. *J. Am. Chem. Soc.* **1985**, *107*, 2388-2393.

(101) Huang, X.; Buchwald, S. L. *Org. Lett.* **2001**, *3*, 3417-3419.

(102) Jameson, D. L.; Goldsby, K. A. *J. Org. Chem.* **1990**, *55*, 4992-4994.

(103) Zopperllaro, G.; Baumgarten, M. *Eur. J. Org. Chem.* **2005**, 2888-2892.

(104) Ishow, E.; Brosseau, A.; Clavier, G.; Nakatani, K.; Pansu, R. B.; Vachon, J.; Tauc, P.; Chauvat, D.; Mendonca, C. R.; Piovesan, E. *J. Am. Chem. Soc.* **2007**, *129*, 8970-8971.

(105) Alvarez, R.; Mehl, G. H. *Tetrahedron Lett.* **2005**, *46*, 67-68.

(106) Huszthy, P.; Kontos, Z.; Vermes, B.; Pinter, A. *Tetrahedron* **2001**, *57*, 4967-4975.

(107) Ruiz-Molina, D.; Wurst, K.; Hendrickson, D. N.; Rovira, C.; Veciana, J. *Adv. Funct. Mater.* **2002**, *12*, 347-351.

(108) Ruiz-Molina, D.; Veciana, J.; Wurst, K.; Hendrickson, D. N.; Rovira, C. *Inorg. Chem.* **2000**, *39*, 617-619.

(109) Sanyal, A.; Chatterjee, S.; Castineiras, A.; Sarkar, B.; Singh, P.; Fiedler, J.; Zalis, S.; Kaim, W.; Goswami, S. *Inorg. Chem.* **2007**, 8584-8593.

(110) Soliman, A. A.; Saadia, A.; Orabi, A. *Spectrochim. Acta, Part A* **2006**, *65*, 841-845.

(111) Toth, A.; Floriani, C.; Pasquali, M.; Chiesi-Villa, A.; Gaetani-Manfredotti, A.; Guastini, C. *Inorg. Chem.* **1985**, *24*, 648-653.

(112) Karam, A. R.; Catarí, E. L.; López-Linares, F.; Agrifoglio, G.; Albano, C. L.; Díaz-Barrios, A.; Lehmann, T. E.; Pekerar, S. V.; Albornoz, L. A.; Atencio, R.; González, T.; Ortega, H. B.; Joskowics, P. *Appl. Catal., A* **2005**, *280*, 165-173.

(113) Willison, S. A.; Hershel, J.; Antonelli, R. M.; Rennekamp, J. M.; Eckert, N. A.; Bauer, J. A. K.; Connick, W. B. *Inorg. Chem.* **2004**, *43*, 2548-2555.

(114) Tang, R.; Wong, K.; Zhu, N.; Yam, V. W. *Dalton Trans.* **2009**, *20*, 3911-3922.

(115) Garcia, M. A. M.; Gelling, A.; Noble, D. R.; Orrell, K. G.; Osborne, A. G.; Sik, V. *Polyhedron* **1996**, *15*, 371-379.

(116) Franklin, B. R.; Herrick, R. S.; Ziegler, C. J.; Cetin, A.; Barone, N.; Condon, L. R. *Inorg. Chem.* **2008**, *47*, 5902-5909.

(117) Lazarova, N.; James, S.; Babich, J.; Zubieta, J. *Inorg. Chem. Comm.* **2004**, *7*, 1023-1026.

(118) Alberto, R.; Egli, A.; Abram, U.; Hegetschweiler, K.; Gramlich, V.; Schubiger, P. A. *J. Chem. Soc., Dalton Trans.* **1994**, *19*, 2815-2820.

(119) Wei, L.; Babich, J.; Zubieta, J. *Inorg. Chim. Acta* **2005**, *358*, 3691-3700.

(120) Casanova, M.; Zangrando, E.; Munini, F.; Iengo, E.; Alessio, E. *Dalton Trans.* **2006**, *42*, 5033-5045.

(121) Bessel, C. A.; See, R. F.; L., J. D.; Churchill, M. R.; Takeuchi, K. J. *J. Chem. Soc., Dalton Trans.* **1991**, *11*, 2801-2805.

VITA

Monica Irais Villa was born in Ciudad Juarez, Chihuahua, Mexico. She graduated from Michael. E DeBakey High School for Health Professions in Houston, Texas in the year 2000. She obtained a Bachelor of Arts degree in English from Grinnell College in Grinnell, Iowa in 2004. A year later, she completed a Bachelor of Arts in chemistry from Simpson College in Indianola, Iowa. For two years, she was employed as an HIV Outreach Coordinator and Clinic Assistant for Planned Parenthood of Greater Iowa. She entered the graduate program in chemistry at the University of Texas at Austin in the fall of 2006.

villa.monica.i@gmail.com

This thesis was typed by Monica Irais Villa.